People's Democratic Republic of Algeria

Ministry of Higher Education and Scientific Research

Echahid Hamma Lakhdar University - El Oued

Faculty of Technology

Department of Process Engineering & Petrochemistry

Dissertation

ACADEMIC MASTER

Domain: Science and Technology

Division: Chemical Engineering

Specialty: Chemical Engineering

Presented by:

1. Imen BENDJEBAR

2. Meriem SADANI

Entitled:

Understanding the corrosion inhibitory action of some organic molecules: DFT, SAR, MD and GUSAR approaches

Dissertation Submitted in Partial Fulfillment of the Requirements for the Master Degree in Chemical Engineering

Publicly defended in: 14/06/2026

Board of Examiners :

Dr. KAOUTHAR Ahmouda	**Chairman**
Dr. Salah Eddine HACHANI	**Supervisor**
Dr. ISSAM Boudouh	**Examiner**

Academic Year : 2025/2026

ACKNOWLEDGEMENTS

We would like to express our sincere gratitude and appreciation to our professor, for their invaluable support and guidance throughout the completion of our thesis. Their expertise, encouragement, and dedication have been instrumental in helping us overcome challenges ***and successfully finalize this work. We are deeply grateful for their commitment to our*** *academic growth and for the insights they provided, which greatly enriched our research. This achievement would not have been possible without their mentorship. Thank you for your constant support and invaluable contributions.*

DEDICATION

To those whose prayers were the light that illuminated my path...

To the first person who taught me how to face life, and how faith and hard work are the path to success...

To those who stayed up all night to help me reach where I am today...

To my caring mother and great father, the source of my strength and pride, I dedicate this humble fruit of a long journey filled with diligence and hard work.

To my brothers and sisters, you are my true support and inexhaustible motivation...

To my colleagues and friends who shared my journey of learning and supported me through every moment of doubt and fatigue, my gratitude and appreciation are indescribable.

To my esteemed professors who never held back their knowledge and guidance, you were beacons illuminating the path...

To everyone who planted hope in my heart, even with a single word, and who had an impact on this journey, thank you from the bottom of my heart.

I dedicate this work to everyone who believed in me... and to myself, who persevered and fought until the end.

BENDJEBARE Imane

DEDICATION

In the name of God, the Most Gracious, the Most Merciful,

With pride and honor, and with a heart brimming with loyalty and devotion, I dedicate this fruit of my labor to those who have had the greatest impact on my life:

To my generous parents, who planted in my heart a love of knowledge and taught me that ambition is not limited by circumstances, and that prayer is my provision on every journey.

To my brothers and sisters, and my companions, who brightened my days with their sincere words, their supportive hearts, and their smiles in moments of fatigue.

To the people of Gaza, to the land that produces men and sparks heroism.

To those who endure under siege, steadfast in their soil like a mountain.

To those who teach the nation that dignity cannot be bought, and that freedom cannot be granted, but rather taken away.

SAADANI Meriem

Abstract:

Density Functional Theory (DFT) calculations were carried out to investigate both the global and local reactivity descriptors of the studied molecules. These theoretical analyses were complemented by structure–activity relationship (SAR) investigations and molecular dynamics (MD) simulations to provide a comprehensive understanding of the corrosion inhibition mechanism. The computational study focused on two arylfuran derivatives, namely 5-(4-bromophenyl)furan-2-carbaldehyde (M1) and 5-(4-chlorophenyl)furan-2-carbaldehyde (M2), with the aim of elucidating the correlation between their electronic characteristics and their inhibitory performance toward mild steel corrosion in acidic media. In addition, toxicity assessments were performed to evaluate their potential effects on human health and the environment. The theoretical findings obtained from the global reactivity parameters, SAR analyses, and MD simulations were found to be in close agreement with the available experimental data, thereby confirming the effectiveness of the investigated compounds as corrosion inhibitors. Furthermore, Fukui function analysis provided valuable insight into the molecular adsorption process by identifying the most reactive atomic centers involved in electron donation and electron acceptance during interaction with the metal surface. Toxicological predictions revealed that both compounds possess relatively low toxicity profiles and limited environmental hazards, highlighting their potential as environmentally acceptable corrosion inhibitors that comply with current safety and sustainability considerations.

Keywords: DFT, global and local reactivity, Fukui, SAR, MD, toxicity, M1, M2.

الملخص:

أُجريت حسابات **نظرية دالة الكثافة (DFT)** لدراسة كلٍّ من واصفات التفاعلية العالمية والمحلية للجزيئات المدروسة. واستُكملت هذه التحليلات النظرية بدراسات **العلاقة بين البنية والنشاط (SAR)** ومحاكاة **الديناميكا الجزيئية (MD)** بهدف تقديم فهم شامل لآلية تثبيط التآكل. وقد ركزت الدراسة الحاسوبية على مشتقين من الأريل فيوران، وهما **-5(4-بروموفينيل)فيوران-2-كربالدهيد (M1)** و**-5(4-كلوروفينيل)فيوران-2-كربالدهيد(M2)** ، بهدف توضيح العلاقة بين خصائصهما الإلكترونية وكفاءتهما في تثبيط تآكل الفولاذ الطري في الأوساط الحمضية. بالإضافة إلى ذلك، أُجريت تقييمات للسمية لتحديد آثارهما المحتملة على صحة الإنسان والبيئة. وقد أظهرت النتائج النظرية المستخلصة من معاملات التفاعلية العالمية، وتحليلات العلاقة بين البنية والنشاط، ومحاكاة الديناميكا الجزيئية توافقًا وثيقًا مع البيانات التجريبية المتاحة، مما يؤكد فعالية المركبين المدروسين كمثبطات للتآكل. علاوةً على ذلك، وفّر تحليل **دالة فوكوي (Fukui)**فهمًا أعمق لعملية امتزاز الجزيئات على السطح المعدني، من خلال تحديد أكثر المراكز الذرية نشاطًا المشاركة في منح الإلكترونات واستقبالها أثناء التفاعل مع سطح المعدن. كما كشفت التنبؤات السمية أن كلا المركبين يتمتعان بمستوى منخفض نسبيًا من السمية وبمخاطر بيئية محدودة، مما يبرز إمكانيتهما كمثبطات تآكل صديقة للبيئة ومتوافقة مع متطلبات السلامة والاستدامة الحديثة.

الكلمات المفتاحية :نظرية دالة الكثافة(DFT) ، التفاعلية العالمية والمحلية، دالة فوكوي، العلاقة بين البنية والنشاط(SAR) ، الديناميكا الجزيئية(MD) ، السمية، M1، M2.

List of Tables

List of Figures

List of Abbreviations

Abbreviation	Meaning
DFT	Density Functional Theory
HF	Hartree Fock
PBE	Pedrew-Bruk-Ernezrhof
B3LYP	Becke, 3-parameter, Lee–Yang–Parr
HOMO	Highest Occupied Molecular Orbital
LUMO	Lowest Unoccupied Molecular Orbital
SAR	Structure-Activity Relationship
MD	Molecular Dynamics
GUSAR	General Unrestricted Structure-Activity Relationships
COSMO-RS	Conductor-like Screening Model for Real Solvents

Table of Contents

General introduction

General introduction

Mild steel is one of the most widely used metallic materials in industry due to its high malleability, low cost, and remarkable mechanical properties. It finds numerous applications in the storage and transport of chemical substances, as well as in various industrial structures. However, when exposed to aggressive environments, particularly acidic or saline ones, this material undergoes corrosion that can alter its physical and mechanical properties, leading to a significant reduction in its performance and lifespan [1].

To limit the destructive effects of corrosion, the use of organic inhibitors at low concentrations is one of the most effective and economical protection methods. The choice of these compounds depends not only on their inhibitory efficacy but also on environmental, toxicological, and economic criteria. The most effective organic inhibitors generally contain heteroatoms such as nitrogen, oxygen, or sulfur, which have lone pairs of electrons capable of interacting with the metal surface. The presence of conjugated π systems also promotes electron transfer mechanisms between the inhibitor molecule and the metal. Furthermore, a planar or near-planar molecular structure enhances adsorption by increasing coverage of the metal surface and strengthening interfacial interactions [2].

The evaluation of corrosion inhibitor efficacy traditionally relies on several experimental methods, including electrochemical impedance spectroscopy (EIS), polarization measurements, mass loss gravimetric analysis, and surface characterization techniques such as scanning electron microscopy (SEM). These methods provide important information on the electrochemical and morphological behavior of materials. However, their implementation often requires expensive equipment, relatively lengthy experimental protocols, and does not always allow for a precise explanation of the molecular mechanisms responsible for the inhibition phenomenon [3].

The development of computational approaches has significantly strengthened the role of theoretical chemistry in the study of corrosion phenomena. In addition to experimental investigations, molecular modeling allows for a detailed exploration of adsorption mechanisms, charge exchange, and the relationships between molecular structure and inhibitory activity. These approaches contribute to a better understanding of anti-corrosion mechanisms while improving the predictive capabilities of studies [4].

Among the most widely used theoretical methods, density functional theory (DFT) plays a crucial role in the analysis of corrosion inhibitors. This method allows for the study of the electronic structure of molecules and the determination of various descriptors of global and local reactivity. These parameters provide valuable information regarding the molecules' ability

to donate or accept electrons, their chemical reactivity, and the nature of the interactions established with the metal surface. Thus, DFT is a particularly effective tool for interpreting experimental results and explaining observed inhibitory performance [5].
Structure-activity relationship (SAR) analysis also represents an important approach in the rational design of new inhibitors. This method aims to establish correlations between the structural properties of molecules and their corrosion protection efficacy in order to identify the molecular parameters responsible for optimal performance. This approach facilitates the prediction and optimization of new compounds with improved protective capabilities [7].

Molecular dynamics (MD) simulations are computer simulations that model the behavior of atoms and molecules over time. These simulations can be used to study the interactions between inhibitors and metal surfaces, which can provide insights into the mechanisms of corrosion inhibition. MD simulations can be particularly useful for investigating the effectiveness of corrosion inhibitors at the atomic and molecular level. By simulating the behavior of the inhibitor molecules in the presence of a metal surface, researchers can observe how the inhibitor molecules interact with the surface and how these interactions affect the rate of corrosion [8].

In addition to inhibitory efficacy, the toxicity of the compounds used has become a major concern in the field of corrosion. Toxicological evaluation is essential to ensure human safety and reduce the environmental impacts associated with the use of chemical inhibitors. In this context, environmental regulations and sustainable development requirements encourage the design of compounds that are both effective and environmentally sound. Early prediction of toxicological properties thus allows for guiding the structural modifications necessary for the development of safer and more environmentally friendly inhibitors [8].
In a recent study, S. Satarkar and R. S. Dubey synthesized two furan derivatives: 5-[4-bromophenyl]-furan-2-carbaldehyde (M1) and 5-[4-chlorophenyl]-furan-2-carbaldehyde (M2). The inhibitory behavior of these compounds against mild steel corrosion in a 0.1 N HCl solution was studied using various electrochemical and analytical techniques, including electrochemical impedance spectroscopy and polarization curves [9].
The experimental results obtained revealed that compound M1 has a higher inhibitory efficacy than compound M2. Despite the interest of these experimental observations, the theoretical mechanisms explaining this difference in efficacy remain insufficiently explored. This study relies on density functional theory (DFT) calculations, combined with SAR analysis, to examine the influence of the electronic and structural properties of molecules on their anticorrosion

activity at the molecular level. Furthermore, the ProTox and GUSAR predictive platforms are used to estimate the potential toxicological effects of these compounds on human health and the environment. This integrated theoretical approach aims to deepen our understanding of the inhibition mechanisms and contribute to the rational development of effective, sustainable, and environmentally friendly corrosion inhibitors.

Chapter I: State-of-the-art review of corrosion and protection methods.

I.1. Introduction:

This first chapter is devoted to the general study of the corrosion phenomenon, presenting its fundamentals, its factors, its main types, and its consequences. Furthermore, particular attention is paid to the experimental methods commonly used for evaluating and characterizing corrosive processes. Finally, the main protection and prevention strategies developed to limit the degradation of metallic materials are presented and discussed. The chapter concludes with a summary of the essential concepts covered.

I.2. Definition of corrosion:

Corrosion is defined as the physicochemical interaction between a metal and its surrounding environment, leading to changes in the metal's properties and often functional degradation of the metal itself. Another definition considers this phenomenon to be simply the the thermodynamic tendency of metals to return to more stable oxidized forms [10].

I.3. Corrosion impacts:

Many people have already encountered, directly or indirectly, corrosion in various forms, including rust formation on iron barriers, the degradation of steel structures, and the progressive deterioration of ships and their equipment. Another area particularly susceptible to this phenomenon is piping systems. This includes, among other things, water pipes in homes, where corrosion develops primarily from the inside, as well as underground pipelines transporting water, gas, and oil across different regions [11].

Thus, it is reasonable to assume that most people have at least a basic understanding of corrosion, a phenomenon that can be broadly defined as the degradation of a material, usually metallic, or its properties, resulting from its interaction with the surrounding environment. This definition highlights the fact that not only can materials deteriorate, but also their functional properties. In some types of corrosion, the loss of mass or the visible signs of degradation are minimal or even imperceptible. However, internal changes can alter the mechanical properties of the material, leading to sudden and unpredictable failures. These transformations sometimes render assessment methods based solely on visual inspection or mass variation insufficient [11].

In today's industrial and economic climate, companies cannot afford significant corrosion-related failures, especially when they result in material damage, loss of life, unplanned production shutdowns, or environmental pollution. Therefore, considerable efforts are being made to control and limit corrosion from the manufacturing stages and throughout the entire lifecycle of equipment, particularly in sectors handling highly corrosive substances. Indeed, corrosion can cause critical failures in industrial infrastructure and equipment, leading to high repair costs, product loss or contamination, significant environmental impacts, and risks to

personnel safety. Therefore, decisions regarding the durability of a structure or its components are based on a rigorous assessment of the conditions influencing corrosion and its degradation kinetics [11].

I.4. Corrosion factors:

Corrosion phenomena depend on a large number of factors, the main ones being [12]:

- **Factors of the corrosive environment:** concentration of the reactant, oxygen content, and pH of the environment.
- **Metallurgical factors:** alloy composition, heat and mechanical treatment.
- **Factors defining the conditions of use:** surface condition, part shape, type of inhibitor, and assembly processes.
- **Time-dependent factors:** aging, mechanical stresses, and changes in protective coatings.

I.5.I.5. Main corrosion mechanisms:

The corrosion of a metal or alloy can develop through different processes, each of which characterizes a specific type of corrosion. Three types of corrosion can be distinguished:

I.5.1. Chemical corrosion:

Chemical corrosion is generally understood as corrosion that does not involve the passage of an electric current between the solid and the gas and/or liquid. It is a heterogeneous reaction between a solid phase and a gaseous or liquid phase. In the case where the reactant is gaseous (this is the case with oxygen, which has been the most studied), a dry corrosion phenomenon occurs. If the reactant is a liquid, the metal is attacked, forming a corrosion product on its surface [13].

I.5.2. Electrochemical corrosion:

This is corrosion where the areas constituting the anodes are attacked when an electric current flows between the anodes and cathodes. This type of corrosion can be caused by heterogeneity in either the metal or the reactant. The existence of heterogeneity determines the formation of an electric cell. Metals are generally not single-phase. When immersed in a reagent, they are therefore most often subject to electrochemical corrosion [14].

I.5.3. Bacterial corrosion:

This can be defined as the sector of corrosion in which processes are accelerated by microorganisms without altering the basic electrochemical phenomenon. Most cases of biocorrosion occur under biofilms and can take various forms in terms of the materials and microorganisms involved [15].

I.6. Corrosion morphology:

To solve a corrosion problem affecting a structure, it is essential to characterize it by identifying the form in which it takes hold. Several types of corrosion have been identified; the two most common forms are presented below:

I.6.1. Uniform or generalized corrosion:

Generalized corrosion is the most widespread form of corrosion. This form of corrosion is characterized by a chemical or electrochemical reaction that occurs uniformly on the surface exposed to the corrosive environment. This type of corrosion is usually expected for parts that are part of a structural element that may be sacrificed over time, but it affects all common metals [16].

Figure I.1: Uniform corrosion [16].

I.6.2. Localized corrosion:

Localized corrosion is a form of degradation that develops in restricted areas of the metal surface, while the rest of the material remains relatively intact. Unlike uniform corrosion, it causes very intense attack at specific points, which can lead to rapid perforation of the structure despite a low overall mass loss [17].

Pitting corrosion is one of the most common manifestations of localized corrosion; therefore, Figure I.2 is identified as pitting corrosion while illustrating the localized corrosion mechanism.

Figure I.2: Pitting corrosion [17].

I.7. Laboratory studies on corrosion:

Laboratory corrosion studies rely on several experimental methods designed to evaluate the behavior of metallic materials in aggressive environments. These techniques are divided into destructive and non-destructive methods, allowing for the acquisition of quantitative and qualitative information on corrosion mechanisms and the effectiveness of inhibitors.

I.7.1. Destructive techniques:

I.7.1.1. Weight loss method:

The gravimetric method consists of measuring the mass change of a metallic sample before and after immersion in a corrosive environment for a specified duration. The corrosion rate is calculated from the mass loss, the exposed surface area, and the immersion time. This simple and rapid technique is widely used despite its limited accuracy [18].

I.7.1.2. Potentiodynamic polarization:

Potentiodynamic polarization is an electrochemical method used to determine essential parameters such as the corrosion potential, the corrosion current density, and the Tafel slopes. It provides valuable information on anodic and cathodic mechanisms as well as on the corrosion rate of metallic materials [19].

I.7.2. Non-destructive techniques:

I.7.2.1. Open-circuit potential (OCP):

Open-circuit potential involves measuring the evolution of the electrochemical potential of a metal without current flow. This technique allows for monitoring system stability, passivation phenomena, and the action of corrosion inhibitors over time [20].

I.7.2.2. Electrochemical impedance spectroscopy:

Electrochemical impedance spectroscopy (EIS) is a highly effective method for studying metal/solution interfaces and protective coatings. Nyquist and Bode plots allow for the evaluation of corrosion resistance, coating durability, and inhibitor effectiveness [21].

I.7.2.3. Electrochemical frequency modulation:

Electrochemical frequency modulation (EFM) is a non-destructive method capable of directly determining corrosion kinetic parameters without relying on Tafel constants. It is based on the simultaneous application of two sinusoidal signals of different frequencies [22].

I.7.2.4. Electrochemical noise analysis:

Electrochemical noise measures the natural current and potential fluctuations produced by corrosion reactions. This fast and sensitive technique provides detailed information on the mechanisms and kinetics of corrosion processes [23].

I.7.2.5. Surface morphology analysis:

Surface analysis techniques allow observation of corrosion damage and evaluation of protective mechanisms. Scanning electron microscopy (SEM) reveals the morphological state of corroded surfaces, while electron spectroscopy (EDS) provides information on elemental composition. Atomic force microscopy (AFM) allows the study of roughness and topography at the nanoscale. Finally, X-ray photoelectron spectroscopy (XPS) is used to identify the chemical composition and electronic state of surface layers [24].

I.8. Corrosion protection:

The cost incurred by the annual degradation of materials has led to the implementation of protection methods. In terms of corrosion protection, it is possible to act on the material itself (judicious choice, suitable shapes, etc.), on the surface of the material (coating, painting, any type of surface treatment, etc.) or on the environment with which the material is in contact (corrosion inhibitors). The most effective method of corrosion prevention is the appropriate selection of the metal or alloy according to the conditions to which it will be subjected [25].

I.8.1. Application of coatings:

To prevent anodic and cathodic reactions from occurring, the metal can be isolated from the corrosive environment using coatings, which are commonly classified into two main families [26]:

- Metallic coatings, which can be anodic or cathodic.
- Non-metallic coatings (paints, resins, plastics...).

I.8.2. Protective oxides:

Protective oxides are compact and adherent oxide films that reduce corrosion by limiting the direct contact between the metal and the aggressive environment. Typical examples include alumina (Al_2O_3) on aluminum and chromia (Cr_2O_3) on stainless steels. These films are associated with passivation and can markedly decrease the corrosion rate when they remain continuous and stable. However, their protective efficiency can decrease in the presence of defects, cracks, chloride ions, or mechanical damage, which may locally break the passive layer and initiate localized corrosion [27].

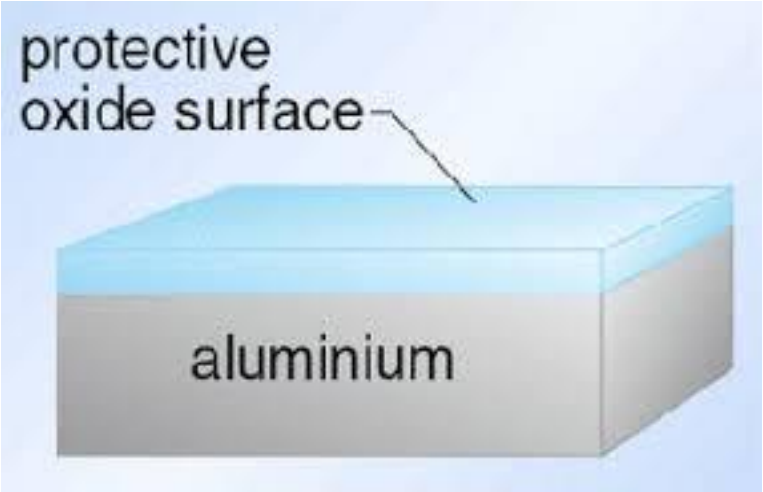

Figure I.3: Deposited oxide layer to protect aluminum [27].

I.8.3. Cathodic protection:

Cathodic protection is an electrical process that, through a permanent modification of the electrical potential of the protected steel, makes it possible to achieve a significant reduction of the corrosion rate. It is a corrosion prevention technique that transforms the entire pipeline into the cathode of a corrosion cell. Cathodic protection is a process of great importance that has enabled the large-scale development of high-pressure steel pipelines for the transport of liquid or gaseous hydrocarbons [28].

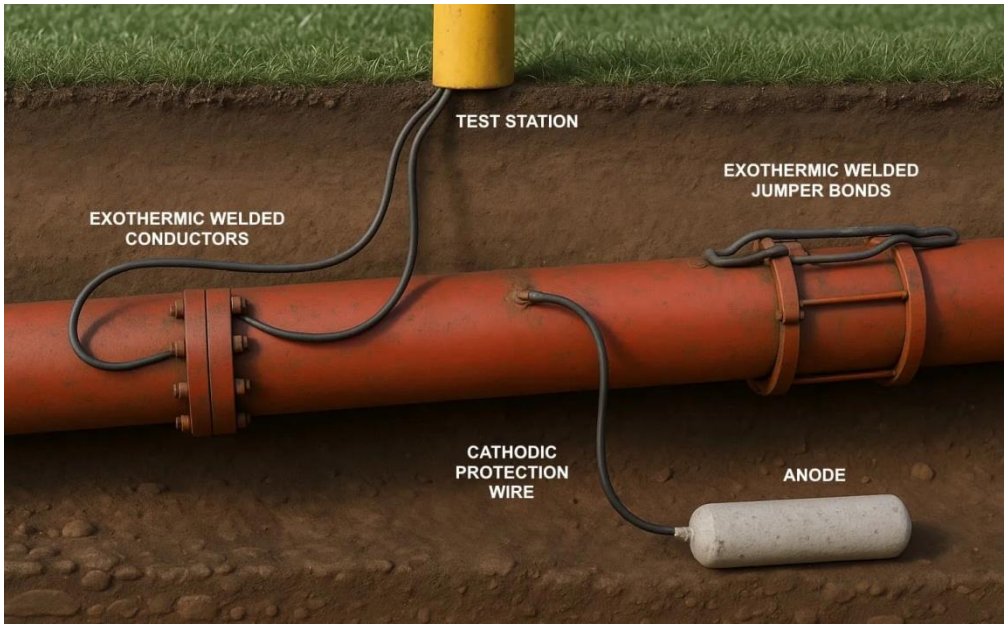

Figure I.4: Cathodic protection [28].

I.8.4. Anodic protection:

Anodic protection is an electrochemical corrosion prevention technique that involves polarizing a metal at a controlled anodic potential to maintain it in its passive range. Within this range, a stable, compact, and adherent oxide layer forms on the metal's surface, significantly limiting its dissolution and thus reducing the corrosion rate. This method relies on the passivating behavior of certain metals, such as stainless steel and titanium, and requires precise potential control to prevent the transition to the transpassive range where corrosion can reappear. It is particularly useful in highly corrosive environments, notably in the chemical industry (sulfuric acid, reactors, tanks), but remains limited to materials capable of passivation and requires a reliable electrochemical control system [29].

I.8.5. Corrosion inhibitors:

The use of corrosion inhibitors has become essential to limit the attack on metallic materials. However, the methods used to inhibit corrosion must be evaluated according to the specific parameters of the system, because preventive measures used successfully in one environment may be detrimental under other conditions. The originality of this method lies in the fact that the anti-corrosion treatment is not carried out on the metal itself, but through the corrosive environment [30].

Inhibition delays electrode reactions such as charge transfer or mass transport, and especially the corrosion process. This is achieved through the use of chemical substances known as corrosion inhibitors.

I.8.5.1. Definition of a corrosion inhibitor:

A corrosion inhibitor is a substance that mitigates corrosion when added to an environment in low concentrations.

In practical terms, an inhibitor is generally effective at low concentration because it modifies the kinetics of the anodic dissolution reaction, the cathodic reduction reaction, or both, without causing a major change in the bulk corrosive medium.

I.8.5.2. Characteristics of corrosion inhibitor:

Generally, a corrosion inhibitor should meet the following criteria [30]:

- Reduce the corrosion rate of a metal without altering its physicochemical properties, particularly its mechanical strength.
- Remain stable in the presence of other environmental components, especially oxidants.
- Be economical.
- Withstand operating temperatures.
- Be effective at low concentrations.
- Comply with non-toxicity standards.

I.8.5.3. Classification of corrosion inhibitors:

I.8.5.3.1. According to their Chemical Composition:

I.8.5.3.1.1. Organic corrosion inhibitors:

Organic inhibitors constitute the most widely used category in corrosion control. Their molecular structure generally contains heteroatoms such as nitrogen, sulfur, or oxygen, capable of interacting with the metal surface. Sulfur compounds often exhibit greater effectiveness than nitrogen compounds due to sulfur's greater capacity to donate electrons.

One of the main advantages of these inhibitors lies in their high effectiveness, even at low concentrations. Their inhibitory power generally increases with the molecular mass of the molecule. Furthermore, organic inhibitors are currently preferred over inorganic inhibitors due to their more limited environmental impact.

The functional groups that promote their adsorption onto the metal are primarily amine (-NH_2), mercapto (-SH), hydroxyl (-OH), and carboxyl (-COOH) groups. Many industrially used organic inhibitors are also derived from petroleum industry by-products, which reduces their production cost [31].

I.8.5.3.1.2. Inorganic corrosion inhibitors:

Inorganic inhibitors are mainly used in alkaline media and are rarely used in acidic solutions. In solution, these compounds dissociate into ions, whose anions and cations provide the inhibitory action.

Among the most common inorganic inhibitors are chromates, molybdates, silicates, and phosphates. Despite their effectiveness, the use of several of these substances is now heavily regulated due to their harmful effects on the environment [31].

I.8.5.3.2. According to their mode of action:

I.8.5.3.2.1. Passivating inhibitors:

Passivating inhibitors act by forming a three-dimensional protective film between the metal surface and the corrosive environment. These compounds, also called interphase inhibitors, integrate into barrier layers and promote the formation of compact, homogeneous, and low-porosity networks, thus ensuring good material stability [31].

Two categories are generally distinguished:

- Oxidizing ions, such as chromates CrO_4^{2-}, capable of passivating steel even in the absence of oxygen.
- Non-oxidizing ions, such as MoO_4^{2-}, WO_4^{2-}, PO_4^{3-}, $B_4O_7^{2-}$, or $C_6H_5COO^-$, which require the presence of oxygen. Their action is based on promoting oxygen adsorption onto the metal surface, thereby shifting the cathodic reduction reaction. Since these ions are gradually consumed, regular monitoring of their concentration in industrial circuits remains necessary [31].

I.8.5.3.2.2. Adsorption inhibitors:

Adsorption corresponds to the binding of inhibitor molecules to the metal surface without major chemical transformation [31]. This phenomenon results from the fact that the atoms present on the surface possess incomplete bonds, which gives them a strong tendency to attract neighboring species. The interaction between the inhibitor and the metal can be of two types: physisorption and chemisorption.

Physisorption (physical adsorption) preserves the chemical identity of the adsorbed molecules. It relies primarily on weak interactions such as:

- Van der Waals dispersion forces;
- Electrostatic interactions due to electric fields;
- Hydrogen bonds involving hydroxyl or amine groups.

In this case, the adsorbed molecules readily interact with the metal surface but can also detach rapidly. When the metal has a positive charge, such as iron in an acidic environment, the adsorption of anionic species is favored.

Chemisorption, on the other hand, involves the formation of chemical bonds between the inhibitory molecule and the metal surface. This interaction results from the sharing or transfer of electrons, particularly from lone pairs on atoms such as O, N, S, or P. The bonds thus formed are more stable and generally lead to irreversible adsorption [31].

This mechanism profoundly alters the electronic distribution of the adsorbed molecules and produces an effective blocking effect on the metal surface. Although slower than physisorption, chemisorption generally provides better protection against corrosion [31].

The efficiency of adsorption also depends on several parameters, including:

- The molecular structure of the inhibitor.
- The charge density at the metal surface.
- The nature of the electrolyte.
- The compactness of the adsorbed layer.
- The interactions between adsorbed molecules.

The formation of organometallic complexes on the metal surface can also contribute to strengthening the inhibitory power [17].

I.8.5.3.2.3. Cathodic inhibitors:

Cathodic inhibitors reduce the rate of the cathodic reaction, which leads to a shift in the corrosion potential towards lower values. Their action thus slows down the electrochemical processes responsible for metal degradation [32].

I.8.5.3.2.4. Anodic inhibitors:

Anodic inhibitors are primarily inorganic compounds such as orthophosphates, silicates, or chromates. Their mechanism consists of increasing the corrosion potential until a passivation zone is reached, where a stable protective film forms on the anodic surface of the metal [32].

I.8.5.3.2.5. Mixed inhibitors:

Mixed inhibitors act simultaneously on the anodic and cathodic reactions. They reduce the global corrosion rate while causing only a small variation in the corrosion potential [32].

I.9. Conclusion:

Corrosion is not only an inevitable natural phenomenon; it also represents a major economic, environmental, and safety challenge. Its consequences can lead to considerable financial losses, ecosystem degradation, and industrial accidents that endanger people and facilities.

Understanding corrosion mechanisms remains essential for selecting the most suitable materials, industrial processes, and protection methods. An effective prevention strategy relies on the judicious choice of control and analysis techniques to optimize the performance of protection systems.

In practice, the study of corrosion often requires combining several experimental methods to precisely identify the mechanisms involved. However, the correct interpretation of the observed electrochemical phenomena remains the fundamental element for establishing long-term protection.

In the industrial sector, continuous corrosion monitoring using appropriate techniques allows for the early detection of equipment degradation and the implementation of corrective measures before critical damage occurs.

Among the most widely used protection solutions is the use of corrosion inhibitors, which slow the rate of metal degradation to an acceptable level. However, increasingly stringent environmental regulations concerning their synthesis, use, and disposal have spurred the development of safer and more environmentally friendly inhibitors.

Therefore, current research is primarily focused on the design of durable, effective, and environmentally sound corrosion inhibitors capable of meeting modern industrial requirements while minimizing their environmental impact.

This need justifies the transition toward computational methods, which can help interpret inhibitor reactivity, adsorption behavior, and structure–activity relationships before more extensive experimental validation.

Chapter II: Quantum computational methods

II.1. Introduction:

This chapter presents the quantum chemical methods used to interpret molecular reactivity and physicochemical phenomena. It presents the Schrödinger equation and the main methods for solving it, addressing the various approximations and approaches used in quantum calculations. Furthermore, global and local reactivity descriptors are developed in detail to better understand the mechanisms of chemical reactivity. Finally, this chapter concludes with a concise presentation of the calculation software used in this study.

II.2. Quantum chemistry:

Quantum chemistry is a branch of theoretical chemistry that uses the principles and equations of quantum mechanics to describe and predict the behavior of chemical systems at the atomic and molecular scale [33].

II.3. Importance of quantum chemistry:

Quantum chemistry is a fundamental discipline of modern chemistry based on the application of the principles of quantum mechanics, particularly the Schrödinger equation, to the study of atomic and molecular systems. It allows us to interpret, at the microscopic scale, the structural, electronic, and energetic properties of chemical species. Thanks to this theoretical approach, it becomes possible to understand reaction mechanisms as well as the behavior of molecules and materials under different physicochemical conditions [33].

The main areas of interest in quantum chemistry can be summarized as follows:

Understanding chemical reactions:

Quantum chemistry provides powerful tools for analyzing reaction mechanisms. It allows us to evaluate energy barriers, transition states, and the kinetic and thermodynamic parameters of reactions. These studies contribute to the optimization of chemical processes and the development of more selective and efficient catalysts [33].

Determination of molecular structure:

Quantum methods allow for the precise calculation of molecular geometric parameters, such as bond lengths, valence angles, and electron distributions. Studying these characteristics facilitates the interpretation of the physicochemical properties of compounds, including their polarity, stability, solubility, and reactivity [33].

Study of material properties:

Quantum chemistry plays a crucial role in analyzing the electronic, mechanical, and thermal properties of materials. It contributes to the design of innovative materials with characteristics suited to various technological applications, such as electronic devices, energy storage systems, catalysts, and magnetic materials [33].

Modeling of complex chemical systems:

Quantum approaches enable the simulation of highly complex chemical systems, including enzymatic reactions, intermolecular interactions, and gaseous or condensed phase processes. These simulations provide a better understanding of chemical phenomena and facilitate the optimization of experimental conditions [33].

Drug design and development:

In the pharmaceutical field, quantum chemistry plays a crucial role in studying the interactions between bioactive molecules and their biological targets. It enables the evaluation of the stability, reactivity, and potential activity of chemical compounds, thus contributing to the rational design of more effective and safer drugs [33].

Corrosion research:

Quantum chemistry plays a crucial role in the study of corrosion by enabling the analysis of the electronic properties of molecules and their interactions with metallic surfaces. It contributes to understanding the adsorption mechanisms of corrosion inhibitors, predicting their effectiveness, and identifying the active sites responsible for metal protection. Thanks to quantum computing, it becomes possible to design new, more efficient, and more environmentally friendly inhibitors, while also complementing experimental results [33].

II.4. Schrödinger's equation:

Consider a quantum mechanical system composed of N electrons and N nuclei. To determine its fundamental physical properties such as the total energy E and the many-body wave function Ψ, which fully describes the electronic and nuclear degrees of freedom it is necessary to solve the time-independent Schrödinger equation, originally formulated by Erwin Schrödinger in 1925 [34].

The equation is expressed as:

$$H\Psi = E\Psi \quad (II.1)$$

Where:

H = Hamiltonian operator (total energy of the system).

Ψ = Wave function (describes the quantum state).

E = Energy eigenvalue.

However, Time-Dependent Schrödinger equation describes the dynamic evolution of a system.

Hamiltonian operator can be decomposed into kinetic and potential energy contributions as follows:

$$H = T_e + T_n + V_{ee} + V_{ne} + V_{nn} \qquad (II.2)$$

Where:

$T_e = -\sum_i^N \frac{h^2}{2m} \nabla_i^2$ *:* is the kinetic energy of the electrons.

$T_n = -\sum_A^{N_\alpha} \frac{h^2}{2M_A} \nabla_A^2$: is the kinetic energy of atoms.

$v_{ee} = \frac{1}{2}\sum_i^N \sum_{j\neq i}^N \frac{e^2}{|\overrightarrow{r_i}-\overrightarrow{r_j}|}$: is the electron-electron interaction potential.

$v_{ne} = -\sum_i^N \sum_A^{N_\alpha} \frac{z_A e^2}{\overrightarrow{r_i}-\overrightarrow{R_A}}$: is the nucleus-electron interaction potential.

$v_{nn} = \frac{1}{2}\sum_A^{N_\alpha} \sum_{B\neq A}^{N\alpha} \frac{z_A z_B e^2}{|\overrightarrow{R_A}-\overrightarrow{R_B}|}$: is the nucleus-nucleus interaction potential.

We can write the Hamiltonian H in the form:

$$H = -\sum_i^N \frac{h^2}{2m} \nabla_i^2 - \sum_A^{N_\alpha} \frac{h^2}{2M_A} \nabla_A^2 + \frac{1}{2}\sum_i^N \sum_{j\neq i}^N \frac{e^2}{|\overrightarrow{r_i}-\overrightarrow{r_j}|} - \sum_i^N \sum_A^{N_\alpha} \frac{z_A e^2}{\overrightarrow{r_i}-\overrightarrow{R_A}} + \frac{1}{2}\sum_A^{N_\alpha} \sum_{B\neq A}^{N\alpha} \frac{z_A z_B e^2}{|\overrightarrow{R_A}-\overrightarrow{R_B}|} (II.3)$$

In this formulation, r_i and R_A denote the position vectors of electrons and nuclei, respectively, while Z_A represents the atomic number of nucleus A [35].

II.5. Solution of the Schrödinger equation:

The Schrödinger equation is the fundamental equation of quantum mechanics that describes the temporal and spatial evolution of the wave function of a quantum system. This equation is only analytically solvable for very simple systems (hydrogen atom, H_2^+ ion). For real systems, we use approximations.

II.5.1. Approximations:

II.5.1.1. Born-Oppenheimer approximation:

The Born-Oppenheimer approximation is a key simplification used to solve the molecular Schrödinger equation. It is based on the fact that nuclei are much heavier than electrons and

therefore move much more slowly. This allows the electronic and nuclear motions to be treated separately [36].

Under this approximation, the total wave function is written as a product of an electronic part and a nuclear part:

$$\Psi(r,R) \approx \psi e(r;R)\, \chi n(R) \quad \text{II.4}$$

Where:

- r represents the electronic coordinates,
- R represents the nuclear coordinates,
- ψe(r;R) is the electronic wave function parametrically dependent on fixed nuclear positions,
- χn(R) is the nuclear wave function describing nuclear motion on a potential energy surface.

The electronic Schrödinger equation is solved with fixed nuclear positions to obtain an energy that depends on nuclear coordinates. This energy is then used as a potential energy surface for solving the nuclear motion problem. This separation greatly simplifies quantum chemical calculations.

The Hamiltonian can thus be defined as:

$$H = H_e + H_n \quad \text{(II.5)}$$

Where H_e and H_n denote the electronic and nuclear Hamiltonians, respectively, subsequently the electronic Schrödinger equation is written:

$$He = -\sum_i^N \frac{h^2}{2m} \nabla_i^2 - \sum_i^N \sum_A^{N_\alpha} \frac{z_A e^2}{|\overrightarrow{r_i} - \overrightarrow{R_A}|} + \frac{1}{2} \sum_i^N \sum_{j \neq i}^N \frac{e^2}{|\overrightarrow{r_i} - \overrightarrow{r_j}|} \quad \text{(II.6)}$$

Or else:

$$He = \sum_i^N h_{i+\frac{1}{2}} \sum_i^N \sum_{j \neq i}^N \frac{e^2}{|\overrightarrow{r_j} - \overrightarrow{r_j}|} \quad \text{(II.7)}$$

Where hi is the one-electronic Hamiltonian.

The electronic Schrödinger equation can then be written as follows:

$$H_e \psi_e = E_e \psi_e \quad \text{(II.8)}$$

II.5.1.2. Hartree-Fock approximation:

The Hartree-Fock (HF) approximation is a fundamental method used to obtain approximate solutions of the many-electron Schrödinger equation. It is based on replacing the complex electron-electron interactions by an average mean-field potential experienced by each electron [37].

In this approach, the many-electron wave function is expressed as a single Slater determinant constructed from one-electron spin orbitals, ensuring the antisymmetry required by the Pauli exclusion principle. The electronic problem is then reduced to a set of coupled one-electron equations, known as the Hartree-Fock equations

In the HF framework, the electronic wave function is approximated by a single Slater determinant:

$$\psi^{HF} = (x_1, x_\Sigma, \dots, x_N) = \frac{1}{\sqrt{N!}} \begin{vmatrix} \phi_1(x_1)\phi_2(x_2)\cdots\phi_N(x_1) \\ \phi_1(x_2)\phi_2(x_2)\cdots\phi_N(x_2) \\ \cdots \\ \cdots \\ \phi_1(x_N)\phi_2(x_N)\cdots\phi_N(x_N) \end{vmatrix} \qquad \text{(II.9)}$$

Where $\frac{1}{\sqrt{N!}}$ is the normalization constant of this wave function, $\phi i(j)$ denotes the ith spin monoelectron orbital and (j) indicates the spatial and spin coordinate of electron $j$grouped in the variable

The orbital spins are given by the product of an orbital function $\phi i(r_j)$ and a spin function $\alpha(\sigma_j)$ where

$$\sigma = \pm\frac{1}{2}\begin{cases} spin\alpha(\uparrow)\sigma = \frac{1}{2} \\ spin\beta(\downarrow)\sigma = \frac{-1}{2} \end{cases} \quad \text{(II.10)}$$

The spin functions α and β obey the condition of orthonormality:

$$\langle\alpha|\alpha\rangle = \langle\beta|\beta\rangle = 1 \wedge \langle\alpha|\beta\rangle = \langle\beta|\alpha\rangle = 0 \qquad \text{(II.11)}$$

The Slater determinant satisfies the principle of antisymmetry because it changes sign if two rows or two columns are swapped. Swapping two rows amounts to changing the space and spin

coordinates of the electron pair. We therefore have the property of antisymmetry with respect to this exchange.

The spin $\phi_i(r_i)$ orbitals are the solutions to the Hartree-Fock equation:

$$F\phi_i(x_i) = \varepsilon_i\phi_i(xi) \qquad \text{(II.12)}$$

Where F is the Hartree-Fock operator defined for an electron by

$$F = \frac{-h^z}{zm}\nabla_i^2 + v_{ext} + V^{HF} \qquad \text{(II.13)}$$

Where V^{HF} is the Hartree-Fock potential, which represents the potential applied to electron i by the other electrons. This potential is expressed using two operators, J and K [59].

$$V^{HF} = \sum_i^N J_i(x_1) - k_i(x_1) \qquad \text{(II.14)}$$

With:

$$j_i(x_1)|\phi_j(x_1) \geq \left(\int \phi_i\ (x_2)\frac{1}{|\vec{r_2}-\vec{r_1}|}\phi_i(x_2)\,dx_2\right) \vee \phi_j(x_1) > \qquad \text{(II.15)}$$

Where $j_i(x_1)|$is the Coulomb operator representing the average repulsion potential exerted by an electron located in ϕ_i on electron 1.

$$ki(x_1)|\phi_i(x_1) \geq \left(\int \phi_i\ (x_2)\frac{1}{|\vec{r_2}-\vec{r_1}|}\phi_i(x_2)\,dx_2\right)/\phi_i\,(x_1) > \qquad \text{(II.16)}$$

Where $k_i(x_1)$is the exchange operator which comes from the anti-symmetric nature of the wave function, and has no classical equivalent: the action of$k_i(x_1)$ on $\phi_j(x_1)$causes the exchange of electron 1 with electron 2.

These equations are solved iteratively in a self-consistent field (SCF) procedure, where the electron density is updated until convergence is reached. Although electron correlation beyond the mean-field description is not explicitly included, the Hartree–Fock method provides a useful first approximation and serves as a starting point for more advanced post-HF methods [37].

II.5.2. Numerical methods:

The Schrödinger equation thus forms the mathematical foundation of all computational quantum chemistry.

II.5.2.1. Density Functional Theory (DFT):

Density functional theory is a quantum chemical method that allows the electronic structure of molecular systems to be studied with reasonable accuracy and computational cost. It is widely used in computational quantum chemistry, condensed matter physics, and materials science. The conceptual basis of DFT was introduced through the Thomas–Fermi model and later formalized by the Hohenberg–Kohn theorems [38]. According to the first theorem, the external potential, and therefore the ground-state properties, are uniquely determined by the electron density. The second theorem states that the ground-state energy obeys a variational principle with respect to the electron density [39].

II.6. Hybrid functionals:

From the 1990s onwards, in parallel with experimentation, new approximations appeared and provided energies, structures and molecular properties. These approximations consist of adding a non-local exchange term from the Hartree-Fock method to the Kohn-Sham type exchange-correlation functional.

The first of these, the B3 functional proposed by Becke in 1993, paved the way for models such as the widely used B3LYP. More recently, the work of Zhao and Truhlar (M06-2X, M06-HF…) has led to the development of even more accurate functionals, particularly for energy calculations.

B3LYP is a widely used hybrid exchange-correlation functional in DFT. It combines Becke's three-parameter exchange functional with the Lee–Yang–Parr correlation functional and includes a fraction of Hartree–Fock exchange. This formulation has made it useful for the calculation of molecular structures and electronic properties relevant to corrosion inhibition studies [40].

The B3LYP exchange-correlation energy is as follows:

$$\boldsymbol{EXCB3LYP} = \boldsymbol{EXCLDA} + (\boldsymbol{EXHF} - \boldsymbol{EXLDA}) + (\boldsymbol{EXGGA} - \boldsymbol{EXLDA}) + (\boldsymbol{ECGGA} - \boldsymbol{ECLDA}) \quad \text{II.17}$$

The subscripts X and C denote the exchange and correlation energies, respectively.

This method has some limitations, such as:

• Underestimation of energy barrier heights.

• Standard B3LYP poorly describes dispersion interactions unless appropriate dispersion corrections are included.

Despite these drawbacks, this method remains relatively effective and the basis for calculations for most chemical compounds.

II.7. Basis functions [41]:

The artificial wave functions used in Kohn-Sham DFT are represented as a set of Kohn-Sham molecular orbitals, each of these orbitals being a linear combination of the basis functions, χ(r):

$$(\boldsymbol{r}) = \sum \boldsymbol{c}(\boldsymbol{r})\boldsymbol{k}\boldsymbol{v}=\mathbf{1} \qquad \text{II.18}$$

With:

: is the index of the basis functions.

: is the total number of basis functions.

: is a coefficient that represents the contribution of each basic atomic orbital to the molecular orbital. These are coefficients adjusted during the optimization of the wave function for minimizing electronic energy. The basis functions themselves remain unchanged.

The different forms of Slater and Gaussian basis functions can be represented in any mathematical form, but some forms are more popular than others. Here are some examples of commonly used bases:

• The 6-31G basis set: core orbitals are represented by a contraction of six Gaussian primitives, whereas valence orbitals are described by a split-valence double-zeta representation. In this context, zeta refers to the number of basis functions used to describe valence orbitals, not to the number of digits in a term.

• **The 6-311G basis set:** is a triple zeta valence basis set. Mono-zeta sets are rarely used because their accuracy is quite low and they are only suitable for fast qualitative calculations. Two other types of functions, allowing for a better representation of heteroatoms, charged or radical systems are added to these bases:

Polarization function:

The polarization function describes the modification of the electron density around a nucleus by allowing atomic orbitals to change shape. It is introduced by adding higher angular momentum functions, such as p-type functions for hydrogen and d-type functions for heavier atoms. These polarization orbitals are commonly denoted by an asterisk (*) in the basis set notation.

b) Diffuse function:

Diffuse orbitals describe the electron density at long distances from the nucleus, especially for charged or radical atoms. They are obtained by adding an orbital of the same type, but with a higher principal quantum number.

To indicate the addition of diffuse orbitals, we add a ++ to the basis in question. Among these bases, we find:

• T**he 6-31+G basis:** diffuse orbitals added to heavy atoms.

• The 6-31++G basis set: diffuse functions are added to both heavy atoms and hydrogen atoms.

II.8. Solvation methods:

In computational quantum chemistry, the study of an isolated molecule is not always sufficient to accurately describe real chemical systems, as the majority of reactions take place in solution. Introducing solvent effects therefore presents a significant challenge in theoretical chemistry, as it involves considerations from statistical mechanics and increases the complexity of the models. To account for these effects, two main families of models are used: discrete models, in which solvent molecules are explicitly treated and allow for the description of local solute-solvent interactions, but at the cost of high computational overhead; and continuous models, in which the solvent is represented as a continuous dielectric medium simulating the average environment of the system [42].

II.8.1. Polarizable Continuum Model (PCM):

The Polarizable Continuum Model (PCM) is a widely used approach for simulating solvation effects due to its numerical efficiency and conceptual simplicity. It avoids the explicit modeling of solvent molecules by representing the solvent as a continuous medium characterized by a dielectric constant. In this framework, the solute is placed in a cavity defined within the continuum, generally constructed from atomic spheres adapted to its geometry, while the interior of the cavity is approximated by a vacuum ($\varepsilon = 1$). The surrounding solvent is described by its actual dielectric constant εs.

The model is based on a self-consistent reaction force (SCRF) approach, in which the solute's electronic distribution polarizes the surrounding medium, which in turn reacts by generating charges on the cavity surface. This iterative process continues until electrostatic convergence is achieved between the solute and the solvent. The total solvation energy then results from the contribution of the solute's electronic energy and the interaction energy with the medium, including electrostatic effects and, in some cases, dispersion and repulsion contributions. In the computational methodology adopted in this study, the PCM model was used is based on the Cancès-Tomasi integral equations, as implemented in the Gaussian software, and allows for an efficient estimation of the solvent's effects on the electronic properties of the systems studied [43].

II.9. Global reactivity descriptors:

The frontier molecular orbital (FMO) theory and the HSAB (Hard and Soft Acids and Bases) principle allow us to understand the reactivity and selectivity of certain chemical systems.

According to Koopmans' theorem [44], the ionization potential (I) is defined as the required energy to remove an electron from a molecule. However, the Electron affinity (A) is defined as

the energy released following the capture of an electron, the quantum parameters can be given by the following equations:

$$I = -E_{\text{HOMO}} \quad \text{(II.19)}$$

$$A = -E_{\text{LUMO}} \quad \text{(II.20)}$$

The energy gap (ΔE) is calculated as follows:

$$\Delta E = E_{\text{LUMO}} - E_{\text{HOMO}}$$

The electronegativity (χ), chemical hardness (η), chemical softness (S), and electrophilicity index (ω) are known as global reactivity descriptors. These indices can be calculated from the energies of the frontier molecular orbitals (HOMO and LUMO) [45]:

$$\chi = \frac{I+A}{2} \quad \text{(II.22)}$$

$$\eta = \frac{I-A}{2} \quad \text{(II.23)}$$

$$\sigma = \frac{1}{\eta} \quad \text{(II.24)}$$

The electrophilicity index (φ) introduced by Parr et al is given as follows [45]:

$$\omega = \frac{\chi^2}{2\eta} \quad \text{(II.25)}$$

The tendency of electron donation from the inhibitor to the metal surface was quantified through the fraction of electrons transferred (ΔN), evaluated using Pearson's electronegativity equalization principle:

$$\Delta N = \frac{\chi_{\text{Fe}} - \chi_{\text{in}}}{2(\eta_{\text{Fe}} + \eta_{\text{in}})} \quad \text{(II.26)}$$

In Eq. (II.26), χFe and χinh correspond to the electronegativities of bulk iron and the inhibitor molecule, respectively, while ηFe and ηinh denote their associated global hardness values. For bulk iron, standard theoretical values of χFe = 7 eV and ηFe = 0 eV were adopted, as commonly assumed in corrosion inhibition studies [45].

The maximum electron transfer parameter (ΔN_{max}) can be calculated as follows:

$$\Delta N_{\text{max}} = \frac{\chi}{2\eta}$$

The back-donation energy ($\Delta E_{b\text{-}d}$) can be quantified using the following equation [45]:

$$\Delta E align lb - d \quad = -\frac{\eta}{4}$$

II.10. Local reactivity parameters [46]:

To analyze the reactivity of a specific atomic site within a molecule, several local descriptors have been proposed, among which electron density is the fundamental parameter. Within the framework of Fukui's frontier orbital theory, the Fukui function was introduced to describe the variation of electron density when the number of electrons changes. It satisfies normalization conditions similar to those of electron density and exhibits discontinuities related to variations in the electronic system, leading to the definition of different functions depending on the type of chemical attack (nucleophilic, electrophilic, or radical).

These functions can be approximated by the finite difference method using the frozen nucleus approximation, which allows for a direct link to the frontier orbitals (HOMO and LUMO), responsible for chemical reactivity. A high value of the Fukui function generally indicates a strong propensity for electron transfer and therefore increased reactivity. To make these concepts applicable to molecular chemistry, we adopt the atom-in-molecule approach, leading to condensed forms on atoms, where q_K represents the atomic electron population determined from population analysis methods such as Mulliken or Hirshfeld. It should be noted that Mulliken analysis can lead to negative values for Fukui functions, which sometimes limits its interpretation, while the Hirshfeld approach generally provides more physically consistent values, although cases of negative values may also have specific chemical significance.

II.11. Molecular dynamics simulation [47]:

Molecular dynamics (MD) simulation is a widely used computational method for studying interactions between molecules at the atomic level, particularly in the field of corrosion inhibitors. Here is a structured overview of how this approach can be applied to study a corrosion inhibitor.

Molecular dynamics simulation allows:

- To observe in detail the adsorption of the inhibitor on the metal surface.
- To predict the physicochemical properties (adsorption, diffusion, interaction energy).
- To analyze the stability of the inhibitor layer.
- To study the effect of different parameters (pH, temperature, concentration, metal type).

II.12. Importance of human and environmental toxicity assessment [48]:

The study of the human and environmental toxicity of corrosion inhibitors has become a crucial aspect of developing new inhibitors, particularly for large-scale industrial applications. Its importance can be summarized as follows:

II.12.1. Protection of human health:

Corrosion inhibitors can come into contact with workers during their manufacture, handling, or use. Some chemical compounds exhibit harmful effects such as:

- Skin and eye irritation.
- Acute or chronic toxicity.
- Mutagenic, carcinogenic, or teratogenic effects.
- Damage to the respiratory, nervous, or hepatic systems.

Evaluating human toxicity therefore allows for the identification of potential risks and the selection of safer molecules for users.

II.12.2. Environmental protection after use:

Corrosion inhibitors can be discharged into industrial wastewater or reach soils and aquatic ecosystems. Some compounds persist in the environment for a long time and can: contaminate water resources:

- Affect aquatic organisms (algae, fish, and crustaceans).
- Accumulate in food chains.
- Disrupt the balance of ecosystems.

Ecotoxicity studies allow us to assess the environmental impact of inhibitors before their industrial use.

II.12.3. Development of green inhibitors:

Toxicological analysis facilitates the design of environmentally friendly corrosion inhibitors (green inhibitors), characterized by:

- Low toxicity to humans.
- High biodegradability.
- Low bioaccumulation.
- Reduced environmental impact.

These properties meet the current requirements of sustainable development and green chemistry.

II.12.4. Compliance with international regulations:

Environmental regulations are becoming increasingly strict regarding the use of industrial chemicals. Toxicity assessment allows us to verify the compliance of inhibitors with international standards relating to the protection of health and the environment.

II.12.5. Optimizing the efficacy-safety ratio:

A highly effective corrosion inhibitor is not necessarily suitable for industrial use if it exhibits high toxicity. Toxicological studies help find a compromise between:

- Corrosion efficacy.
- Human safety.
- Environmental compatibility and economic viability.

II.13. Importance of aqueous solvation in corrosion inhibition [49]:

Solvation water plays a crucial role in the behavior of corrosion inhibitors in aqueous environments. When an inhibitor is introduced into a corrosive solution, its molecules immediately interact with surrounding water molecules to form a solvation layer. This interaction influences several physicochemical properties responsible for inhibitory efficacy.

II.13.1. Influence on corrosion inhibitor solubility:

Good solvation promotes the dissolution and homogeneous dispersion of inhibitor molecules in the corrosive environment. An insufficiently solvated inhibitor may exhibit low solubility, thus limiting its availability to interact with the metal surface.

II.13.2. Effect on transport to the metal surface:

The water molecules surrounding the inhibitor contribute to its movement in the solution. The structure of the solvation layer therefore influences the diffusion of the inhibitor from the solution volume to the metal/solution interface where adsorption occurs.

II.13.3. Influence on the adsorption mechanism:

Before the inhibitor is adsorbed onto the metal surface, the water molecules adsorbed onto the metal often need to be displaced. The efficiency of the process then depends on the competition between:

- Metal-water interactions.
- Metal-inhibitor interactions.
- Inhibitor-water interactions.

An inhibitor capable of efficiently replacing the adsorbed water molecules forms a more stable and compact protective layer.

II.13.4. Impact on protective film formation:

The structure and thickness of the solvation layer influence the orientation of inhibitor molecules during adsorption. This orientation determines the compactness, adhesion, and stability of the protective film formed on the metal surface, which constitutes the primary barrier against corrosive species.

II.14. Programs and Platforms:

II.14.1. HyperChem [50]:

HyperChem is a molecular modeling and computational chemistry software developed by Hypercube, Inc. It allows users to build molecules, simulate their behavior, and analyze their properties using several computational methods:

- Molecular mechanics calculations (force fields such as MM+, AMBER, CHARMM)
- Semi-empirical quantum chemistry calculations (AM1, PM3, PM6, etc.)
- Ab initio and DFT calculations.
- Molecular dynamics and Monte Carlo simulations.

The intuitive graphical interface facilitates 3D visualization of structures, molecular orbitals, and electrostatic surfaces. It is commonly used in research and teaching in organic chemistry, biochemistry, and materials science.

II.14.2. Gaussian [51]:

Gaussian is highly regarded computational quantum chemistry software developed by Gaussian, Inc. It is considered one of the most comprehensive and widely used tools in academic and industrial research for electronic structure calculations.

Main Calculation Methods:

- Hartree-Fock (HF) method.
- Post-Hartree-Fock methods: MP2, MP3, MP4, CCSD….etc.
- Density Functional Theory (DFT): numerous functionals (B3LYP, PBE, M06, etc.).
- Semi-empirical methods: AM1, PM3, PM6…etc.
- Multiconfigurational methods: CASSCF, CASPT2.

Key Features:

- Geometry Optimization and Vibrational Frequency Search.
- Electronic Transition Calculations (TD-DFT, CIS, EOM-CCSD).
- Spectroscopic Properties: IR, Raman, UV-Vis, NMR, EPR.
- Ab Initio and On-the-Fly Molecular Dynamics.
- Gas-Phase and Solution-Phase Calculations (Solvation Models: PCM, SMD, etc.).
- Periodic Calculations for Solids and Surfaces.

II.14.3. Materials Studio [52]:

Materials Studio is a software suite for modeling and simulation at the atomic and molecular scale, developed by BIOVIA Company. It specializes in materials science, chemistry, and biology.

Main modules and methods:

- **CASTEP:** for periodic materials (solids, surfaces, interfaces).
- **DMol³:** Numerical DFT for molecules, solids, and surfaces.
- **Forcite Plus:** Molecular mechanics and molecular dynamics (force fields)
- **GULP:** Simulation of ionic and covalent materials.
- **VAMP:** Semi-empirical quantum chemistry.
- **Amorphous Cell:** Construction of amorphous structures.
- **Adsorption Locator:** Prediction of adsorption sites.
- **Sorption:** Simulation of adsorption and isotherms.
- **Blends:** Prediction of polymer miscibility.

Application areas

- **Inorganic materials:** crystals, ceramics, metals, oxides.
- **Polymers and organic materials:** structure, mechanical properties, miscibility.
- **Catalysis:** surfaces, adsorption, reaction mechanisms.
- **Energy:** batteries, fuel cells, solar panels
- **Pharmaceuticals:** Crystallography, Polymorphism, Formulation

Advantages of Materials Studio:

- Unified graphical interface for all modules.
- Excellent handling of periodic structures (crystal lattices, surfaces, interfaces).
- Automated workflows for screening studies.
- Integration with crystallographic databases.

II.14.4. ProTox III platform [53]:

The ProTox III (ProTox-3.0) platform is an in silico tool for predicting human toxicity, widely used in medicinal chemistry and the safety assessment of chemical compounds. It allows for the rapid estimation of the potential toxicity of molecules based on their structure (SMILES, chemical name, or molecular design), without the immediate need for experimental testing on humans or animals.

ProTox III uses machine learning, molecular similarity, and QSAR approaches to predict several levels of human toxicity, including acute toxicity (LD50), organ toxicity (hepatotoxicity, cardiotoxicity, neurotoxicity, nephrotoxicity), as well as important endpoints such as mutagenicity, carcinogenicity, and immunotoxicity. The platform also provides information on potential biological targets, toxicity pathways (AOP/Tox21), and the overall hazard profile with confidence scores, thus facilitating chemical risk assessment from the earliest stages of molecule design.

Thus, ProTox III is an essential tool in human predictive toxicology, making it possible to reduce experimental testing, accelerate drug development and contribute to a safer and more sustainable approach to chemistry and health.

II.14.5. GUSAR platform [54]:

The GUSAR (General Unrestricted Structure–Activity Relationships) platform is a computer-based tool using QSAR methods to predict the toxicity of chemical compounds from their molecular structure. In the field of environmental toxicity assessment, it is particularly useful for estimating the effects of substances on various aquatic organisms such as fish, Daphnia magna, and algae, as well as their bioaccumulation potential. Through statistical models and molecular descriptors, GUSAR provides rapid preliminary predictions that require experimental validation without the need for immediate in vivo experiments. This tool thus constitutes an effective approach for preliminary ecological risk assessment and aligns with modern green chemistry and environmental protection strategies.

II.15. Conclusion:

Density functional theory (DFT) in computational chemistry has demonstrated its effectiveness as an advanced analytical tool for studying the interaction of inhibitors at the atomic scale, thus enabling the development of innovative solutions that improve inhibitor efficiency without requiring costly laboratory experiments. This approach, which combines experimental research and theoretical analysis, provides a solid foundation for developing corrosion control strategies and meeting the durability and safety requirements of metallic materials in various industrial applications.

Chapter III: Results and discussion.

III.1. Introduction:

This final chapter focuses on establishing a correlation between the experimental results obtained in the corrosion study and the theoretical investigations carried out at the molecular level, in order to better interpret the behavior of the studied inhibitors. First, the selected experimental study is presented in detail. Then, the various theoretical approaches used, including calculations based on density functional theory (DFT), structure-activity relationship analysis (SAR), molecular dynamics (MD) simulations, and the evaluation of human and environmental toxicity, are precisely described. Finally, a thorough analysis of all the results obtained is performed to clarify the role played by each molecule studied in the corrosion inhibition process.

III.2. Experimental background:

S. Satarkar and R. S. Dubey synthesized two furan derivatives: 5-[4-bromophenyl]-furan-2-carbaldehyde (M1) and 5-[4-chlorophenyl]-furan-2-carbaldehyde (M2). The inhibitory efficacy of these compounds against the corrosion of mild steel in an acidic solution (0.1 N HCl) was evaluated using several electrochemical and analytical techniques, including electrochemical impedance spectroscopy and polarization measurements [9].

The reported experimental results showed that compound M1 exhibited greater inhibition efficacy than molecule M2 [9].

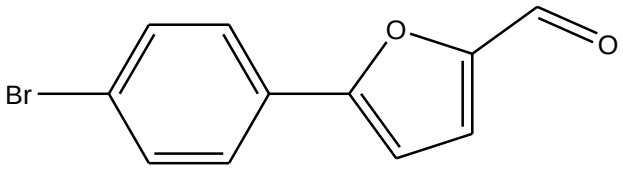

M1

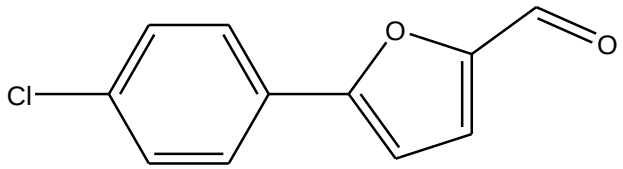

M2

Figure III.1: Molecular structures of the studied corrosion inhibitors.

In this chapter, a complementary theoretical contribution is proposed, drawing on density functional theory (DFT), structure–activity relationship analysis (SAR), and molecular dynamics (MD) simulations. These methods provide detailed information on the electronic properties of the studied inhibitors and offer a better understanding of their mechanism of action in corrosion inhibition. Furthermore, assessing the human toxicity and environmental impact

of these compounds is an essential step to ensure their use under conditions compatible with health and environmental safety requirements.

III.3. Computational details:

To improve reproducibility, the computational workflow is summarized in Table III.1. Software versions were not specified in the source documents and should be completed before final submission if available.

Table III.1: Summary of the computational workflow and main parameters used in the study.

Step	Software / platform	Main method or model	Main parameters	Calculated outputs
Global reactivity	Gaussian / GaussView	DFT/B3LYP	6-31G(d,p); aqueous phase using PCM; convergence criteria and frequency validation to be specified if available	EHOMO, ELUMO, ΔE, μ, I, A, η, S, χ, ω, ΔN
Local reactivity	DMol3 / Materials Studio	Fukui function analysis	DNP basis set; GGA functional as reported	f− and f+ reactive atomic centers
SAR descriptors	HyperChem	Structure–activity relationship descriptors	Descriptor definitions, units, and software version to be specified if available	Polarizability, surface area, molecular volume, hydration energy, LogP
Molecular dynamics	Materials Studio / Discover module	COMPASS force field; NVT ensemble	Fe(110) surface; 298 K; 1 fs time step; 50 ps simulation; Ewald electrostatics;	Adsorption configuration, interaction energy, binding energy, pair

			equilibrium based on energy stabilization	correlation functions
Human toxicity	ProTox-3.0	In silico toxicity prediction	LD50 and GHS-based toxicity classes; prediction probabilities	Acute toxicity, organ toxicity, toxicity endpoints, Tox21 pathways
Environmental toxicity	GUSAR	QSAR-based ecotoxicity prediction	Endpoints for Daphnia magna, Fathead Minnow, Tetrahymena pyriformis, and BCF	Predicted ecotoxicity and applicability domain

III.3.1. Calculation of global reactivity descriptors:

Density functional theory (DFT) is a widely used theoretical method for studying the chemical reactivity of molecules due to its ability to provide optimized geometries and reliable electronic properties of chemical compounds.

In this study, DFT calculations were performed in both the gas and aqueous phases at the theoretical B3LYP level associated with the 6-31G(d,p) basis set. This computational level is recognized for its effectiveness in interpreting the electronic properties of M1 and M2 inhibitors, as well as their inhibitory behavior with respect to corrosion.

The molecular structures of the inhibitors were constructed using GaussView software and then geometrically optimized using Gaussian. To simulate the aqueous environment, the SCRF model based on the polarizable continuum (PCM) approach was applied. This model considers water molecules as a dielectric medium characterized by a dielectric constant of 78.5 [55], thus providing a better representation of solvent-solute interactions. The output files generated by the calculations were then used to determine the various overall reactivity descriptors presented in Chapter II.

III.3.2. Calculation of local reactivity indices:

Local reactivity descriptors were employed to identify the atomic sites within the molecules that are most susceptible to electron donation or acceptance. In this study, the Fukui functions

were calculated using the DMol^3 module implemented in Materials Studio. The calculations were performed with the double numerical polarization (DNP) basis set within the generalized gradient approximation using the Becke-Lee-Yang-Parr functional.

The Fukui indices (f^+ and f^-) were determined from atomic charges or populations using the neutral (N), cationic (N-1), and anionic (N+1) states of the molecules, allowing the identification of the most reactive sites for electrophilic and nucleophilic attacks [56].

For nucleophilic attack: $f^+ = q^A_{N+1} - q^A_N$

For electrophilic attack: $f^- = q^A_N - q^A_{N-1}$

III.3.3. Calculation of structure-activity relationship (SAR) parameters:

The structure-activity relationship (SAR) parameters, including polarizability, molecular surface area, molecular volume, and the Log P partition coefficient, were determined using HyperChem software. These descriptors provide important information on the physicochemical properties of the inhibitors and their ability to interact with the metal surface.

III.3.4. Molecular Dynamics simulation:

To explore the adsorption behavior of inhibitors on the metallic surface at the atomic scale, molecular dynamics simulations were performed using the Discover module. All calculations were carried out under periodic boundary conditions using the COMPASS (Condensed-phase Optimized Molecular Potentials for Atomistic Simulation Studies) force field, known for its ability to accurately describe interactions in condensed systems. The geometries of all system components were optimized beforehand prior to running the simulations [57]. The iron crystal was first generated and then cleaved along the (111) crystallographic plane to construct a surface representative of the metallic substrate. A 6 Å thick layer was used to model the Fe(110) surface. After geometric relaxation using the Smart Minimizer method, the surface was extended into a supercell with dimensions of (10 × 10), thus providing a sufficiently large adsorption area to accommodate the inhibitor molecules. An amorphous cell containing the optimized inhibitors and water molecules was then constructed to reproduce an environment close to real corrosion conditions. During the simulations, the atoms constituting the Fe(110) surface were held immobile, while the inhibitor and water molecules were allowed to move freely in the vicinity of the metal. Non-covalent interactions, including Van der Waals and electrostatic interactions, were evaluated using the Ewald method. The numerical parameters used included a cutoff radius of 15.5 Å, a spline width of 1 Å, and a buffer width of 0.5 Å. Thermal control of the system was achieved using the Andersen algorithm [58]. The simulations

were conducted at a temperature of 298 K in the NVT statistical ensemble (constant number of particles, volume, and temperature), with a time step of 1 fs and a total duration of 50 ps. The trajectories were followed until thermodynamic equilibrium was reached, characterized by the stabilization of the system's energy and thermal fluctuations.

The affinity of the inhibitors for the metallic surface was evaluated by calculating the interaction energy ($E_{interaction}$) and the binding energy ($E_{binding}$), determined from the following relationships [59]:

$$E_{interaction} = E_{total} - (E_{surface} + E_{inhibitor} + E_{solution}) III.1$$

$$E_{binding} = -E_{interaction} III.2$$

Where E_{total} denotes the total energy of the adsorbent/adsorbate system, $E_{surface}$ corresponds to the energy of the iron surface alone, and $E_{solution}$ represents the energy of the medium containing water molecules, while $E_{inhibitor}$ is the energy of the adsorbed inhibitor molecule. A high value for the binding energy reflects a strong interaction between the inhibitor and the metal surface, thus indicating better corrosion protection.

III.3.5. Human toxicity assessment:

In this study, the toxicological profile of the investigated inhibitors was examined using in silico approaches with the ProTox-3.0 platform (https://tox.charite.de/protox3/), a reference tool dedicated to predicting the toxicity of small organic molecules. This platform combines various computational methods, including structural analogy analysis, identification of molecular fragments associated with toxic effects, and machine learning algorithms based on CLUSTER-type models. Through the integration of numerous experimentally validated models, ProTox-3.0 can predict a wide range of toxicological effects, including acute toxicity, potential damage to target organs, specific toxic effects, and interactions likely to affect various biological and cellular pathways listed in the Tox21 program [60].

The hazard level of the studied molecules was assessed based on predicted values of the median lethal dose (LD_{50}). These data were interpreted according to the criteria of the Globally Harmonized System of Classification and Labelling of Chemicals (GHS). Expressed in $mg \cdot kg^{-1}$ of body mass, the LD_{50} values constitute a relevant quantitative indicator for assessing acute toxicity and estimating the potential risks associated with human exposure.

III.3.6. Environmental toxicity assessment:

The potential environmental impact of the studied compounds was analyzed using the GUSAR platform (https://way2drug.com/Gusar/environmental.html), based on QSAR (Quantitative Structure–Activity Relationship) predictive models. This approach makes it possible to

establish correlations between the structural characteristics of the molecules and their biological effects on various aquatic organisms.

Several ecotoxicological parameters were estimated, including the median lethal concentration (LC_{50}) after 96 hours for Pimephales promelas, the LC_{50} after 48 hours for Daphnia magna, and the 50% growth inhibitory concentration (GIC_{50}) for Tetrahymena pyriformis. In addition, the bioconcentration factor (BCF) was calculated to assess the molecules' ability to accumulate in living organisms. Taken together, these indicators provide a comprehensive view of the environmental behavior of the inhibitors and their potential risks to aquatic ecosystems [61].

III.4. Results and discussion:

III.4.1. Global reactivity results:

Figure III.2 shows the optimized molecular structures of the corrosion inhibitors studied, calculated in aqueous phase at the DFT/B3LYP/6-31G(d,p) level of theory.

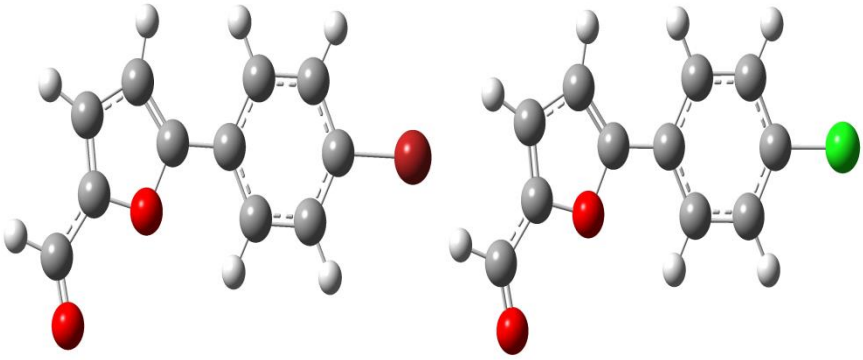

M1 **M2**

Figure III.2: Optimized molecular structures of M1 and M2 in the aqueous phase, calculated at the DFT/B3LYP/6-31G(d,p) level of theory.

The global reactivity indices of the studied corrosion inhibitors were calculated in the aqueous phase and then collected in Table III.2. In what follows, we will discuss the effect of each of the descriptors mentioned in the table on the corrosion inhibition effectiveness.

Table III.2: Global reactivity descriptors of the studied corrosion inhibitors, calculated in the aqueous phase at the DFT/B3LYP/6-31G(d,p) theoretical level.

Parameter	**M1**	**M2**
M	6.0086	6.0376
E_{HOMO}	-6.0208	-6.0376
E_{LUMO}	-2.0655	-2.0594
ΔE	3.9552	3.9782
I	6.9294	6.7253
A	1.8871	1.5536
H	1.9776	1.9891
Σ	0.5057	0.5027
X	4.0431	4.0485
ω	4.1330	4.1200
ΔN	2.9238	2.9354

Note: EHOMO, ELUMO, ΔE, I, A, η, χ, ω, and ΔN are expressed in electronvolts (eV), while μ is expressed in Debye and S is reported as the inverse of hardness according to the convention used in the calculations.

Global reactivity descriptors from quantum chemistry play a crucial role in interpreting and predicting the order of corrosion inhibition yield. They allow for a direct link between the intrinsic electronic properties of inhibitors and their experimental efficacy, moving beyond a purely empirical approach.

Within the framework of density functional theory, these descriptors include, in particular, the frontier orbital energies (HOMO and LUMO), the energy gap, chemical hardness (η), electronegativity (χ), electrophilicity (ω), and the electron transfer fraction (ΔN). Together, they describe a molecule's ability to donate, accept, or redistribute electrons during its interaction with a metallic surface [62].

The main advantage of these parameters is that they allow for predicting the adsorption tendency of inhibitors on the metal, a critical step in the corrosion protection process. For example, an inhibitor with a high HOMO, a low LUMO, and low hardness will be more reactive and will adsorb more readily onto the metal surface, thus forming an effective protective layer. Similarly, high electrophilicity or a high electron transfer fraction can indicate a strengthened electronic interaction with the metal.

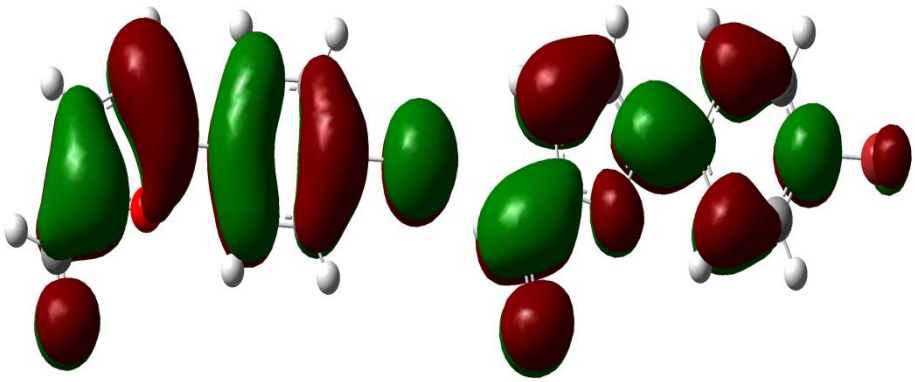

HOMO of M1 **LUMO of M1**

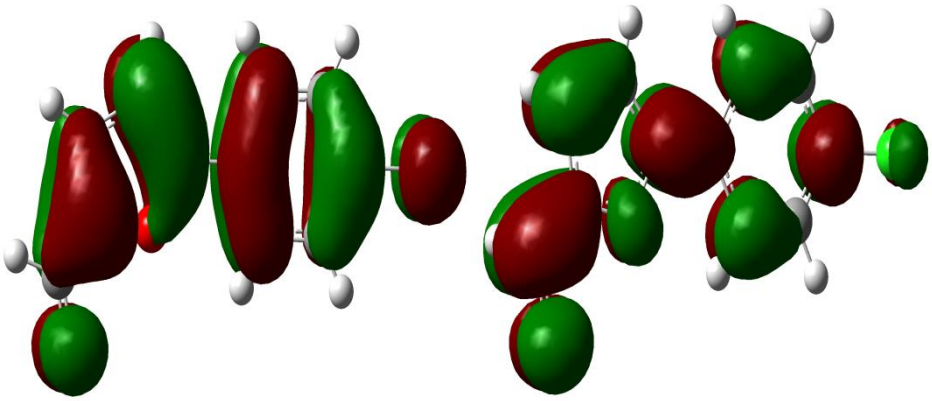

HOMO of M2 **LUMO of M2**

Figure III.3: The electronic distribution of the HOMO and LUMO frontier orbitals across the molecular structures of the examined corrosion inhibitors.

The HOMO/LUMO distributions indicate that the oxygen atoms, the conjugated π system, and the halogen substituents participate in the electronic interaction with the iron surface. Electron donation from oxygen- and π-rich regions to vacant iron orbitals, combined with possible back-donation from iron to low-energy molecular orbitals, supports the adsorption of M1 and M2 on Fe(110).

These descriptors also allow for the establishment of quantitative correlations between electronic structure and inhibition efficiency. This makes it possible to classify inhibitors according to their theoretical effectiveness even before experimental testing. This approach reduces the need for lengthy and costly empirical trials, while improving the understanding of adsorption mechanisms. Frontier orbitals, derived from molecular orbital theory, are a fundamental tool for analyzing the chemical reactivity of inhibitors. They are defined as the highest-energy occupied orbital (HOMO) and the lowest-energy vacant orbital (LUMO). Within the framework of Fukui's frontier orbital theory, these orbitals govern the electronic

interactions between chemical species: the HOMO reflects a molecule's ability to donate electrons, while the LUMO reflects its ability to accept them [63].

The reactivity of an inhibitor is strongly linked to its electronic properties, particularly the energy of its frontier orbitals. A high HOMO energy favors the transfer of electrons to the metal, thus strengthening the molecule's adsorption onto its surface. Conversely, a low LUMO energy facilitates the acceptance of electrons from the metal, contributing to back-donation interactions. These electron exchange mechanisms are essential in the formation of a protective film on the metallic surface [63]. The results given in Table III.2 show that E_{HOMO} obeys the order M1 > M2, this result is in full agreement with the experimental results earlier reported.

A key parameter is the energy gap between the HOMO and LUMO (ΔE). A low ΔE indicates a more polarizable and reactive molecule, thus improving its ability to interact with the metal surface. Conversely, a high ΔE corresponds to greater chemical stability but reduced reactivity. Therefore, inhibitors with a small energy gap are generally more effective [64]. The data collected in Table III.2 show that ΔE is as follows: M1 < M2, this theoretical outcome is in excellent accordance with the order of the corrosion inhibition efficacy earlier reported.

In quantum chemistry, other quantities such as hardness (η) and softness (S) allow for a more refined analysis. Chemical hardness (η) measures a species' resistance to the deformation of its electron cloud. In other words, a hard molecule resists electron transfer and exhibits low polarizability. It is generally associated with high stability and low reactivity. Chemical softness (S) is the inverse of hardness and reflects the ease with which a molecule can exchange electrons. A soft species is highly polarizable, more reactive, and promotes electronic interactions with other systems, particularly metallic surfaces. Low hardness, combined with high softness, indicates a greater capacity to exchange electrons with the metal, thus promoting adsorption and improving inhibitory performance [65]. As displayed in Table III.2, the hardness follows the order M1 < M2 while the softness is as M1 > M2, these results emphasize the order of the experimental inhibition effectiveness earlier reported.

Electronegativity (χ) is a fundamental descriptor in quantum chemistry, describing the ability of an atom or molecule to attract electrons in a chemical bond. This expression shows that electronegativity is linked to the overall electronic distribution of the molecule: the higher the χ, the more the molecule tends to gain electrons; the lower the χ, the more it tends to lose them [66].

In the context of corrosion inhibition, electronegativity plays a key role in the interactions between the inhibitor and the metallic surface. The primary mechanism relies on electron transfer between the inhibitor and the metal. If electronegativity is high, the molecule tends to

capture electrons, which can limit its electron-donating interaction with the metal surface. The electronegativity values, collected in Table III.2, increase as follows: M1 < M2, this result validates the experimental findings previously observed.

Electrophilicity (ω) is a global descriptor in quantum chemistry that measures a molecule's ability to accept electrons. It therefore characterizes the electrophilic nature of a species, that is, its tendency to behave as an electron acceptor during a chemical interaction. A molecule with high electrophilicity has a strong capacity to capture electrons, making it more reactive towards electron donors. Conversely, low electrophilicity corresponds to a lower capacity to accept electrons [67]. Table III.2 demonstrates that M1 has greater electrophilicity than M2, which contradicts the trend reported in the aforementioned experimental work.

The dipole moment is a fundamental quantity in quantum chemistry that measures the separation of positive and negative electrical charges within a molecule. It therefore reflects the unequal distribution of electron densities between atoms. In the field of corrosion inhibition, the dipole moment plays an important role in the effectiveness of inhibitors. A molecule with a high dipole moment exhibits strong polarity, which promotes its interaction with the charged metallic surface and leads to high performance protection [68]. The dipole moment values in Table III.2 follow the sequence M2 > M1, this result does not agree with the order of the inhibition efficiency of the molecules under probe.

The electron transfer fraction from the metal to the inhibitor is an important descriptor in quantum chemistry, used to quantify the electron flow during the inhibitor-metal surface adsorption interaction. It allows us to estimate the extent to which the metal transfers some of its electron density to the inhibitor molecule. The electron transfer fraction is directly related to the effectiveness of inhibitors. A high ΔN value indicates a high electron donation from the inhibitor to the metal surface. This interaction strengthens adsorption on the metal surface, leading to the formation of a compact protective film that limits corrosion [69]. As exhibited in Table III.2, ΔN values decrease following the order M2 > M1, which does not correlate with the experimental data of the studied compounds.

III.4.2. Local reactivity results:

The Fukui functions are local descriptors of reactivity that allow us to locate sites favorable to electron transfer between the inhibitor and the metal. High values of f^- indicate preferred sites for donating electrons to the vacant orbitals of iron, while high values of f^+ correspond to centers capable of accepting electrons from the occupied orbitals of the metal [70]. Table III.3 collects Fukui functions of the corrosion inhibitors under investigation.

Table III.3: Fukui functions of the tested corrosion inhibitors.

M1			**M2**		
Atoms	f^-	f^+	**Atoms**	f^-	f^+
O1	0.031	0.052	O1	0.032	0.053
C2	0.082	0.054	C2	0.085	0.054
C3	0.049	0.083	C3	0.052	0.083
C4	0.076	0.050	C4	0.080	0.049
C5	0.057	0.076	C5	0.060	0.076
C6	0.049	0.123	C6	0.050	0.125
O7	0.081	0.128	O7	0.082	0.132
C8	0.049	0.027	C8	0.050	0.027
C9	0.045	0.041	C9	0.047	0.040
C10	0.038	0.025	C10	0.039	0.026
C11	0.054	0.040	C11	0.058	0.041
C12	0.036	0.026	C12	0.038	0.027
C13	0.045	0.037	C13	0.046	0.037
Br14	0.144	0.060	Cl14	0.111	0.052

For compound M1, the highest values of f^- are observed for the Br14, C2, O7, and C4 atoms. These results show that these centers possess a strong ability to donate their electron density to the iron surface, thus promoting the formation of coordinate bonds with the metal's vacant orbitals. The particularly high value for bromine suggests that this atom plays a major role in the adsorption of the molecule onto the mild steel surface.

Analysis of the f^+ values of compound M1 reveals that the O7 and C6 atoms constitute the main electrophilic sites of the molecule. These centers are the most likely to receive electrons from the filled 3d orbitals of iron through an electron back-donation mechanism. Atoms C3 and C5 also exhibit some electron-donating capacity, contributing to enhanced adsorption interactions between the inhibitor and the metal surface.

A similar trend is observed for compound M2, the highest values of f^- are located on Cl14, C2, O7, and C4, indicating that these atoms represent the main nucleophilic centers involved in electron transfer to the steel surface.

The values of f^+ of compound M2 show that atoms O7 and C6 are the most favorable sites for electron acceptance, followed by C3 and C5 atoms. The presence of high values on the oxygen of the furan core confirms the importance of electron-rich heteroatoms in the adsorption process and in stabilizing the protective layer formed on the surface of the mild steel.

The Fukui function results show that oxygen atoms, carbons of the conjugated π system, and halogens constitute the main active centers responsible for the interaction with the surface of the mild steel. The adsorption of the inhibitors likely occurs via a mixed mechanism involving both electron donation from the nucleophilic centers to the iron and electron back-donation from the metal to the electrophilic centers of the molecule.

The higher value of f^- obtained for the bromine atom in M1 compared to the chlorine atom in M2 suggests that M1 may exhibit a slightly stronger interaction with the metal surface and, consequently, potentially greater inhibitory efficacy.

Overall, the most relevant donor sites follow the order Br14 > C2 ≈ O7 ≈ C4 for M1 and Cl14 > C2 ≈ O7 ≈ C4 for M2, while the strongest electron-acceptor centers are mainly O7 and C6 in both inhibitors. This distinction clarifies the different adsorption contributions of the heteroatoms, halogens, and π-conjugated carbon framework.

III.4.3. SAR results:

Structure-activity relationship (SAR) parameters are a key approach that links the structural characteristics of molecules to their chemical or biological activity, particularly in the field of corrosion inhibition. They encompass several molecular descriptors such as polarizability, the LogP partition coefficient, molecular surface area, molecular volume, and hydration energy.

The main advantage of SAR parameters in corrosion inhibition is their correlation of chemical structure with adsorption efficiency on the metal surface. Indeed, inhibitors act primarily through adsorption, forming a protective layer that limits contact between the metal and the corrosive environment. SAR parameters allow for the identification of structural factors that promote this adsorption. Thus, SARs can explain and predict the order of corrosion inhibition efficiency among different compounds. Molecules exhibiting a favorable combination of these parameters generally show better protective efficiency [71].

Table III.4: SAR parameters of the studied corrosion inhibitors.

Parameter	M1	M2
Polarizability	21.80	21.10
Surface area	392.77	382.75
Volume	612.93	594.14
Hydration energy	9.78	9.76
LogP	-0.41	-0.69

Polarizability is a fundamental property in quantum chemistry that measures a molecule's ability to deform under the influence of an external electric field. In other words, it reflects the ease with which the electron cloud of a chemical species can be displaced relative to the atomic nuclei. A molecule is said to be highly polarizable when its electrons are weakly bound to the nuclei, allowing for a rapid redistribution of electron density in the presence of a charged surface or an electric field. Conversely, low polarizability corresponds to a rigid and relatively inflexible electronic structure [71].

In the field of corrosion inhibition, polarizability plays a crucial role in the adsorption process of inhibitors onto the metal. A highly polarizable molecule can easily adapt its electron distribution upon contact with the metal surface, which promotes the formation of stable adsorption bonds (physical or chemical). This interaction strengthens the coverage of the metal surface by the inhibitor and thus limits contact with the corrosive environment. Therefore, corrosion inhibition efficiency generally increases with the molecule's polarizability [71].

The results presented in Table III.4 show that inhibitor M1 has a slightly higher polarizability (21.80 $Å^3$) than M2 (21.10 $Å^3$). High polarizability promotes the deformation of the molecule's electron cloud during its interaction with the metal surface, thus strengthening donor-acceptor interactions between the electrons of the heteroatoms and the vacant orbitals of the metal. This characteristic suggests that M1 may exhibit stronger adsorption and better protective capacity than M2.

Hydration energy is a thermodynamic quantity in physical chemistry that corresponds to the energy change accompanying the solvation (hydration) of a molecule by water molecules. It therefore reflects the interaction between a chemical species and the aqueous solvent. The hydration energy values given Table III.4 corresponding to the two compounds are very close (9.78 and 9.76 $kcal \cdot mol^{-1}$), demonstrating that their interaction with the aqueous medium is practically identical. Thus, this parameter does not appear to be a major differentiating factor in the expected difference in inhibitory efficacy between the two molecules [71].

In the context of corrosion inhibition, hydration energy indirectly influences the behavior of inhibitors in solution. A highly hydrated molecule interacts strongly with water, which can reduce its ability to adsorb onto the metal surface, as some energy must be expended to break the hydration layer. A good corrosion inhibitor often needs sufficient hydration to ensure its solubility in the aqueous medium, but but not necessarily sufficient to guarantee stronger adsorption onto the metal surface.

Molecular surface area corresponds to the area occupied by a molecule in space, generally defined by the outer shell of its atoms. In quantum chemistry, it constitutes an important structural parameter for describing the size, shape, and accessibility of a molecule. This surface area depends directly on the molecular size, spatial conformation, and arrangement of atoms within the structure [71].

In the context of corrosion, molecular surface area plays a crucial role in the effectiveness of inhibitors. A molecule with a large, flat, and extensive surface area can cover a greater area of the metal surface, thus promoting the formation of a compact and continuous protective film. This limits the contact between the metal and the corrosive environment [71].

Molecular volume is a structural parameter in quantum chemistry that represents the three-dimensional space occupied by a molecule. It corresponds to a measure of the molecule's overall size in space, taking into account the arrangement of its atoms and its conformation.

In the context of corrosion, molecular volume plays an important role in the effectiveness of inhibitors. A molecule with a high volume and an extended structure can cover a larger portion of the metal surface, thus promoting the formation of a dense and continuous protective film. This coverage limits the access of corrosive agents (water, ions, oxygen) to the metal surface [71].

As can be observed in Table III.4, M1 has a slightly larger surface area (392.77 $Å^2$) and volume (612.93 $Å^3$) than M2 (382.75 $Å^2$ and 594.14 $Å^3$, respectively). These values indicate that M1 can cover a larger fraction of the metal surface after adsorption, leading to the formation of a more compact and extensive protective film. Greater surface coverage effectively reduces the number of active sites accessible to corrosive species.

The LogP partition coefficient provides information on the hydrophilic/lipophilic balance of the inhibitors [71]. The negative values obtained for M1 (-0.41) and M2 (-0.69) indicate that both molecules exhibit good affinity for the aqueous medium. However, the less negative value of M1 reveals a slightly more hydrophobic character than that of M2. This property generally promotes the accumulation of molecules at the metal/solution interface and enhances their adsorption onto the metal surface.

Consequently, M1 should form a more stable adsorbed layer that is more resistant to desorption. SAR study highlights that M1 possesses structural characteristics more favorable to corrosion inhibition than M2. Its higher polarizability, larger molecular surface area, greater volume, and slightly more lipophilic nature promote its adsorption onto the metal surface and the formation of an effective protective film. These results therefore suggest that the expected order of inhibitory efficacy is: M1 > M2 This trend is consistent with the generally accepted principles of the structure-activity relationship of organic corrosion inhibitors, according to which high polarizability, large molecular size, and efficient interfacial adsorption contribute to improved inhibitory performance.

III.4.4. MD results:

To further understand the mechanism of action of the studied inhibitors at the molecular level, molecular dynamics (MD) simulations were performed. The most stable adsorption configurations of the neutral arylfuran derivatives on the Fe(110) surface, illustrated in Figure III.4 in lateral and top views, reveal a near-parallel arrangement of the molecules with respect to the metal surface. This planar orientation promotes optimal substrate coverage, thus maximizing the protected surface area and enhancing the inhibitory efficacy of the studied compounds [72].

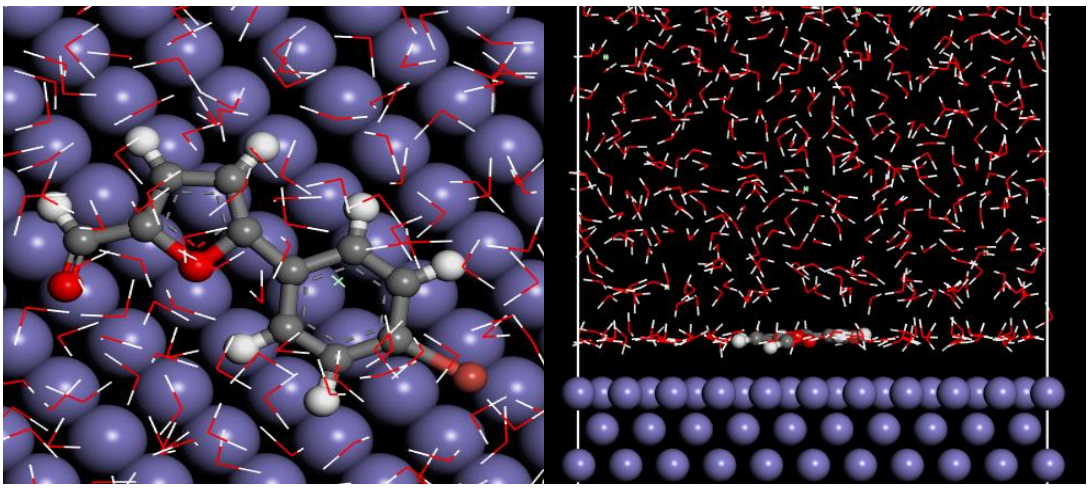

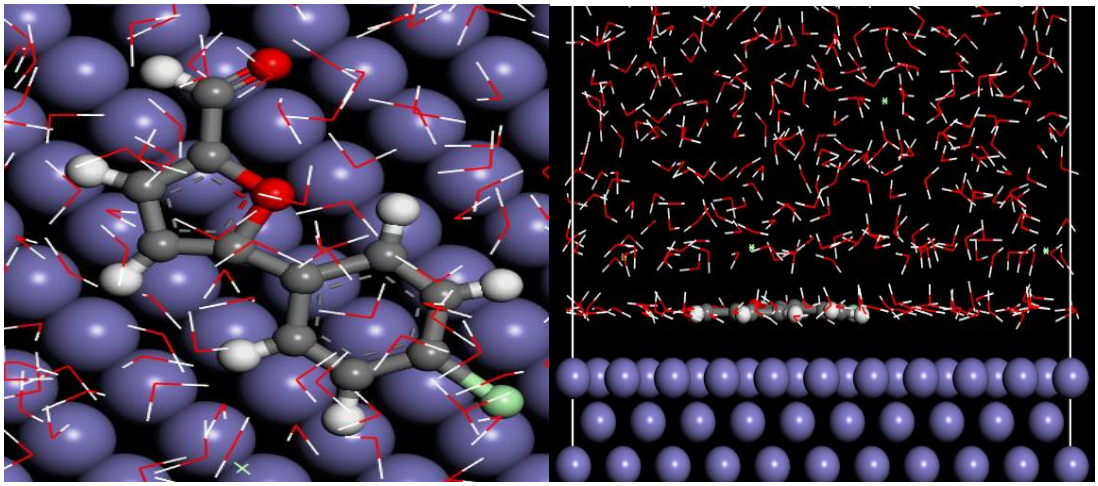

Figure III.4: Equilibrium adsorption configurations of the studied inhibitors on Fe(110) surface obtained by molecular dynamics simulations (top and side views).

The energy parameters from the simulations provide valuable information on the stability of the adsorption process. The negative values of the interaction energies clearly indicate that the adsorption of arylfuran molecules on the iron surface is a thermodynamically favorable and spontaneous phenomenon. Furthermore, the binding energy obeys the order M1 > M2, indicating a stronger interaction between M1 and the metal surface. This trend is perfectly consistent with previously reported experimental results, which attribute superior inhibitory efficacy to M1.

Table III.5: Calculated interaction and binding energies for the adsorption of inhibitors onto Fe(110) surface calculated in aqueous phase (kJ/mol).

System	**Adsorption energy**	**Binding energy**
Fe (110)+M1	-897.25	897.25
Fe (110)+M2	-861.78	861.78

The interaction energy is defined as Einteraction = Etotal − (Esurface+solution + Einhibitor). The binding energy is reported as Ebinding = −Einteraction; therefore, a negative interaction energy indicates a favorable adsorption process, whereas a higher positive binding energy indicates stronger adsorption stability.

The study of pair correlation functions (g(r)) is an effective tool for characterizing the nature of the interactions established between the inhibitor molecules and the metal surface. This analysis allows us to determine the most probable interatomic distances between the active centers of the inhibitors and the iron atoms, thus providing indications of the dominant adsorption mode. In general, the appearance of a g(r) maximum at a distance less than 3 Å is associated with the formation of chemical bonds, reflecting a chemisorption mechanism. Conversely, distances greater than 3.5 Å are generally attributed to physical interactions of the Van der Waals or electrostatic type, characteristic of a physisorption process [73].

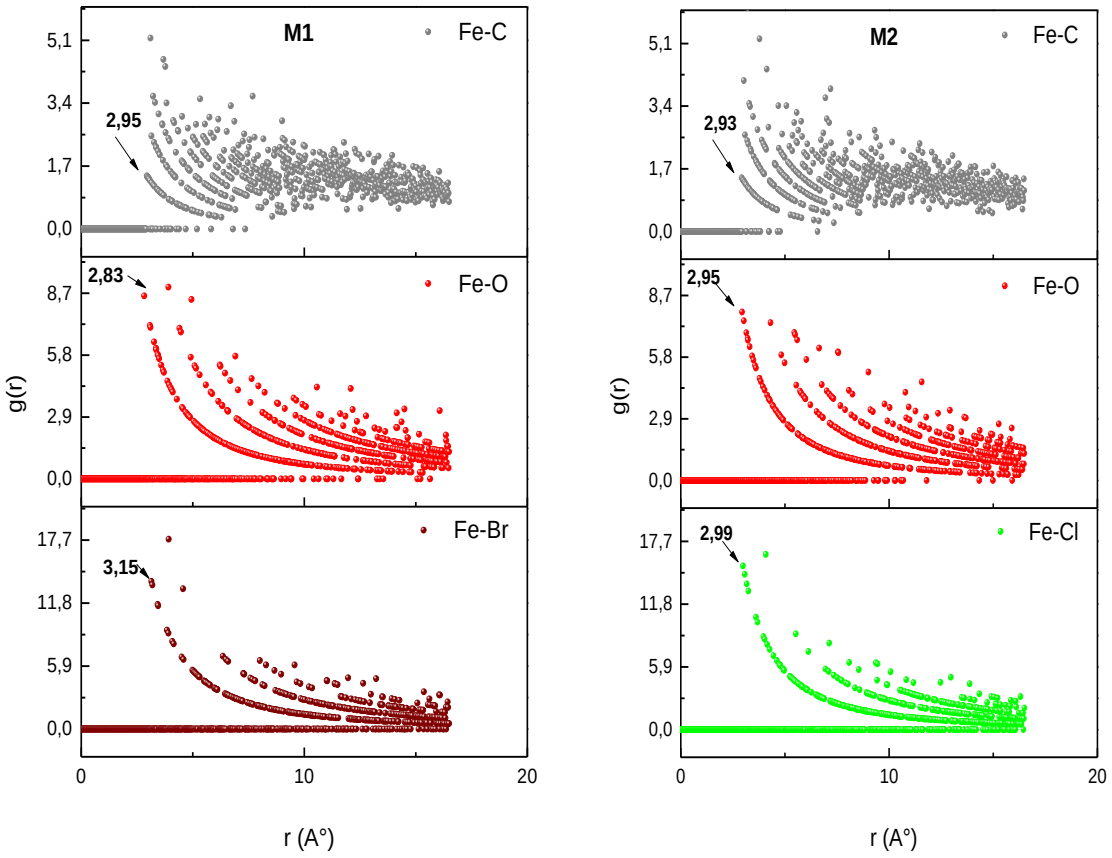

Figure III.5: Pair correlation functions of the Fe-C, Fe-O, Fe-Br, and Fe-Cl pairs for the inhibitors studied.

The curves presented in Figure III.5 show that the initial correlation distances between the iron atoms and the heteroatoms present in the inhibitor molecules (C, O, Br, and Cl) are all less than 3.5 Å. This observation highlights a strong interaction between the inhibitors and the metal surface, dominated by chemisorption phenomena. The formation of such bonds promotes the establishment of a compact and durable adsorbed film, capable of effectively isolating the iron

surface from the corrosive environment and, consequently, significantly improving corrosion resistance.

III.4.5. COSMO-RS profiles:

COSMO-RS profiles are a particularly useful tool for studying the solvation properties and intermolecular interactions of corrosion inhibitors. They allow for the evaluation of charge density distribution at the molecular surface and the identification of regions likely to interact with the corrosive environment and the metal surface [74].

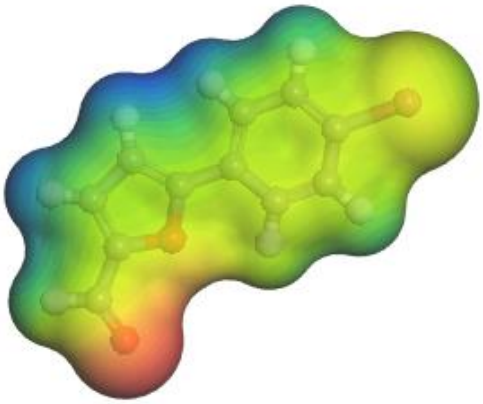

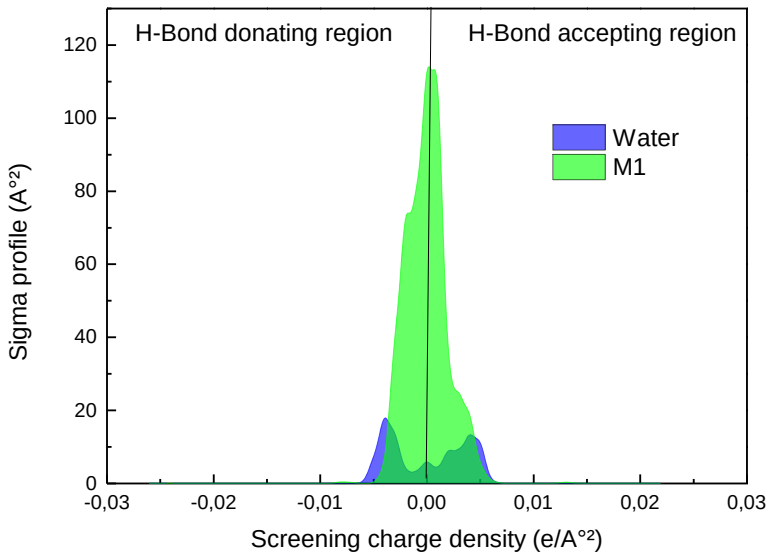

M1

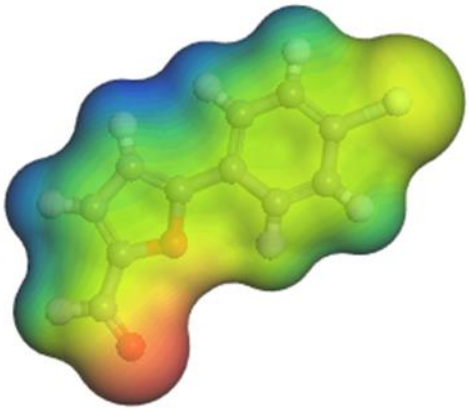

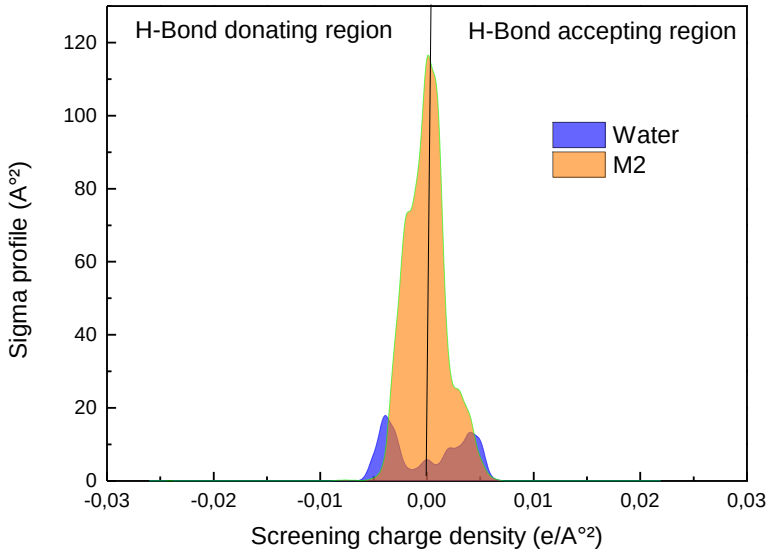

M2

Figure III.6: COSMO-RS profiles for evaluating the solvation properties of M1 and M2 corrosion inhibitors.

As can be seen from Figure III.6, highly electronegative regions are primarily located around heteroatoms, especially oxygen, which constitute the main active centers of the molecule. These sites exhibit a high affinity for electrophilic species present in the environment and can also participate in the adsorption process on the metal surface through electron transfer or sharing. Conversely, electropositive regions can interact with nucleophilic species in the environment, thus contributing to the stability of the adsorbed layers.

The simultaneous presence of hydrophilic and hydrophobic domains gives both inhibitors an amphiphilic character that promotes their dispersion in water while preserving their ability to adsorb onto the metal surface. Hydrogen-bonding interactions between water molecules and electron-rich centers help stabilize the inhibitors in the corrosive solution and facilitate their transport to the metal/solution interface.

The similarity of the profiles observed for M1 and M2 suggests that the two inhibitors exhibit comparable solvation behaviors. However, slight differences in the extent and intensity of the polar regions can influence their affinity for the solvent and their adsorption capacity on the metal surface. A molecule with a more developed polar surface area is generally characterized by better interaction with the aqueous medium and a greater ability to form a compact protective layer.

In the context of corrosion inhibition, good solvation is an important parameter since it facilitates the transport of inhibitor molecules to the metal surface. The COSMO-RS results thus indicate that M1 and M2 possess favorable solvation properties in water thanks to their polar centers capable of establishing strong interactions with solvent molecules. This ability, combined with the presence of electron-donating sites, promotes their adsorption onto the metallic surface and contributes to the observed inhibitory efficacy.

III.4.6. Human health toxicity results:

The human health toxicity assessment of the corrosion inhibitors under investigation was conducted using the ProTox-3.0 predictive platform, with the resulting toxicity parameters presented in Table III.6.

The in silico evaluation of the human toxicity of corrosion inhibitors M1 and M2 reveals an overall acceptable toxicological profile, although some parameters require particular attention. The results show that both molecules exhibit moderate acute toxicity, with estimated LD50 values of 240 $mg \cdot kg^{-1}$ for M1 and 625 $mg \cdot kg^{-1}$ for M2, corresponding to toxicity classes 3 and 4, respectively. These data indicate that M2 is less toxic than M1 and therefore has a better safety profile in the event of accidental exposure.

Regarding organ-specific toxicity, predictions indicate that both inhibitors are non-neurotoxic, non-nephrotoxic, non-cardiotoxic, and non-toxic to the respiratory system, with relatively high probabilities confirming these predictions. These results suggest a low risk of adverse effects on major vital organs. However, M1 exhibits a predicted active hepatotoxicity with a

probability of 0.50, while M2 is classified as inactive with respect to this parameter (0.52), giving the latter an additional advantage in terms of toxicological safety.

Analysis of the various toxicological parameters also shows that both compounds are predicted to be non-immunotoxic, non-mutagenic, and non-cytotoxic, which is a favorable aspect for their potential industrial use. The absence of mutagenic potential suggests, in particular, a low probability of interaction with cellular genetic material, thus reducing the risk of long-term genetic alterations. Nevertheless, both inhibitors are predicted to be potential carcinogens, with probabilities of 0.72 for M1 and 0.69 for M2. Although these results are derived from predictive models and require experimental validation, they indicate that particular attention should be paid to the assessment of their safety before any large-scale application.

Furthermore, M1 and M2 exhibit a high probability of crossing the blood-brain barrier (BBB), with respective probabilities of 0.92 and 0.91. This ability to penetrate the central nervous system can be considered a potential risk factor in the event of prolonged exposure, even though no neurotoxicity was predicted by the models used. Results from the Tox21 signaling pathways also show that both molecules are inactive with respect to the aromatic hydrocarbon receptor (AhR), the estrogen receptor α (ERα), the Nrf2/ARE antioxidant pathway, and the mitochondrial membrane potential (MMP). This lack of activity on these biological targets suggests a low risk of endocrine disruption, oxidative stress, or mitochondrial dysfunction.

The previous toxicological predictions indicate that both inhibitors have a relatively satisfactory safety profile, characterized by low toxicity to most of the organs and biological pathways studied. However, predicted carcinogenicity and the ability to cross the blood-brain barrier are aspects that warrant further experimental investigation. Between the two molecules, M2 appears to be the safer candidate, due to its higher LD50, its lack of predicted hepatotoxicity, and its overall lower toxicity level compared to M1.

Table III.6: In silico prediction of the human toxicity of the tested corrosion inhibitors.

Classification	**Target**	**Prediction for M1**	**Probability for M1**	**Prediction for M2**	**Probability for M2**
General toxicity	LD50	240	-	625	-
General toxicity	Toxicity class	3	-	4	-
Organ toxicity	Hepatotoxicity	Active	0.50	Inactive	0.52
Organ toxicity	Neurotoxicity	Inactive	0.51	Inactive	0.50
Organ toxicity	Nephrotoxicity	Inactive	0.6	Inactive	0.59

Organ toxicity	Respiratory toxicity	Inactive	0.82	Inactive	0.83
Organ toxicity	Cardiotoxicity	Inactive	0.62	Inactive	0.65
Toxicity end points	Carcinogenicity	Active	0.72	Active	0.69
Toxicity end points	Immunotoxicity	Inactive	0.99	Inactive	0.99
Toxicity end points	Mutagenicity	Inactive	0.69	Inactive	0.67
Toxicity end points	Cytotoxicity	Inactive	0.50	Inactive	0.75
Toxicity end points	BBB-barrier	Active	0.92	Active	0.91
Toxicity end points	Nutritional toxicity	Inactive	0.60	Inactive	0.64
Tox21-Nuclear receptor signalling pathways	Aryl hydrocarbon Receptor (AhR)	Inactive	0.83	Inactive	0.83
Tox21-Nuclear receptor signalling pathways	Estrogen Receptor Alpha (ER)	Inactive	0.85	Inactive	0.87
Tox21-Stress response pathways	Nuclear factor (erythroid-derived 2)-like 2/antioxidant responsive element (nrf2/ARE)	Inactive	0.93	Inactive	0.92
Tox21-Stress response pathways	Mitochondrial Membrane Potential (MMP)	Inactive	0.84	Inactive	0.81

III.4.7. Environmental toxicity results:

The in silico toxicity profiles of the examined corrosion inhibitors have been evaluated using GUSAR prediction platform, and the results are collected in Table III.7.

Table III.7: In silico assessment of the environmental toxicity of the tested corrosion inhibitors.

Activity	Prediction Value		Applicability Domain	
	M1	**M2**	**M1**	**M2**
Bioaccumulation factor	1.867	2,160	In AD	In AD
Daphnia magna	6.547	5,869	In AD	In AD
Fathead Minnow	-2.647	-2,522	In AD	In AD
Tetrahymena pyriformis	1.865	1,891	In AD	In AD

Note: The values in Table III.7 are QSAR-based in silico predictions. The endpoints, species, units, and risk thresholds should be reported according to the GUSAR output file and should not be interpreted as substitutes for experimental ecotoxicity tests.

According to the results in Table III.7, the in silico environmental toxicity assessment of the two corrosion inhibitors (M1 and M2) shows that they have a relatively favorable ecotoxicological profile, which is an important criterion for their use in industrial applications. The bioaccumulation factor (BCF) obtained for M1 (1.867) and M2 (2.160) remains low, indicating a low tendency to accumulate in aquatic organisms. These values suggest that both compounds present a limited risk of bioaccumulation along the food chain, although M2 shows a slightly higher propensity for bioaccumulation than M1.

Regarding toxicity to Daphnia magna, a reference organism widely used in ecotoxicological studies, the predicted values of 6.547 for M1 and 5.869 for M2 indicate low acute toxicity to this aquatic species. Both inhibitors appear relatively safe for aquatic invertebrates, with M1 exhibiting slightly lower toxicity than M2.

Toxicity assessments for Fathead Minnow fish revealed values of −2.647 for M1 and −2.522 for M2. These results indicate moderate to low toxicity for higher aquatic organisms, with little significant difference between the two molecules. However, M1 appears to have a slightly lower environmental impact.

The values obtained for Tetrahymena pyriformis (1.865 for M1 and 1.891 for M2) also indicate low toxicity to this aquatic microorganism, suggesting that both inhibitors would have only a minor impact on microbial communities in aquatic environments.

Furthermore, the "In AD" (In Applicability Domain) designation for all predictions confirms that the results obtained fall within the validity range of the model used, thus reinforcing their reliability and scientific relevance.

In summary, the environmental toxicity results show that M1 and M2 have an acceptable ecotoxicological profile, characterized by low bioaccumulation and limited toxicity to the aquatic organisms. M1 appears slightly more environmentally friendly due to its lower bioaccumulation potential and slightly lower toxicity to the aquatic species tested. These observations suggest that both molecules can be considered promising corrosion inhibitors from an environmental perspective, with a moderate ecological advantage for M1.

General conclusion

General conclusion

This study combined density functional theory (DFT), structure–activity relationship (SAR) analysis, molecular dynamics (MD) simulations, COSMO-RS solvation analysis, and in silico toxicity assessment to clarify the inhibition mechanism of two arylfuran derivatives, namely M1 and M2, against mild steel corrosion in acidic medium.

The global reactivity descriptors support the experimentally reported order of inhibition efficiency. In the aqueous phase, M1 exhibited a slightly smaller energy gap than M2 (ΔE = 3.9552 eV for M1 and 3.9782 eV for M2), indicating higher molecular reactivity and a greater capacity for electronic interaction with the metal surface. The hardness/softness trend also supports the greater theoretical reactivity of M1.

The local Fukui analysis identified the most active centers involved in adsorption. For M1, the main electron-donating centers were Br14, C2, O7, and C4, while O7 and C6 were the strongest electron-accepting centers. For M2, the main donor centers were Cl14, C2, O7, and C4, with O7 and C6 again acting as the main acceptor sites. These results indicate that adsorption occurs through the combined contribution of heteroatoms, halogen atoms, and the π-conjugated molecular framework.

The SAR descriptors also favored M1. Its higher polarizability (21.80 $Å^3$), larger surface area (392.77 $Å^2$), greater molecular volume (612.93 $Å^3$), and slightly less negative LogP value (−0.41) suggest better interfacial accumulation and more extensive surface coverage than M2.

The MD results confirmed the strong affinity of both inhibitors for the Fe(110) surface. The calculated interaction energies were −897.25 kJ/mol for M1 and −861.78 kJ/mol for M2, corresponding to binding energies of 897.25 and 861.78 kJ/mol, respectively. This indicates a more stable adsorption of M1, in agreement with the experimental inhibition trend.

The COSMO-RS profiles suggest favorable aqueous solvation for both inhibitors, with polar regions mainly located around oxygen atoms and other electron-rich centers. These solvation features can facilitate transport in the corrosive medium while preserving adsorption ability at the metal/solution interface.

The in silico toxicity results should be interpreted as preliminary predictions rather than definitive safety evidence. ProTox-3.0 predicted LD50 values of 240 mg·kg−1 for M1 and 625 mg·kg−1 for M2, corresponding to toxicity classes 3 and 4, respectively. Environmental predictions suggested low bioaccumulation potential, with BCF values of 1.867 for M1 and 2.160 for M2. However, the predicted carcinogenicity and blood-brain barrier penetration require further experimental verification before any practical application.

Overall, the computational results consistently indicate that M1 should act as the more effective corrosion inhibitor, mainly because of its more favorable electronic structure, active adsorption centers, higher surface coverage descriptors, and stronger adsorption energy on Fe(110).

Future work should include experimental validation through electrochemical impedance spectroscopy, polarization measurements, mass-loss tests, SEM/EDS surface characterization, concentration and temperature studies, and simulations on additional iron surfaces. Such work would strengthen the link between theoretical predictions and practical corrosion protection performance.

References

References

[1] M. I. Khan, A. Sarkar, H. K. Mehtani, P. Raut, A. Prakash, M. J. N .V. Prasad, I. Samajdar and S. Parida, Mater. Chem. Phys., 2022, 290, 126623.

[2] A. Bousskri, A. Anejjar, M. Messali, R. Salghi, O. Benali, Y. Karzazi, S. Jodeh, M. Zougagh, E. E. Ebenso and B. Hammouti, J. Molec. Liquids, 2015, 211, 1000–1008.

[3] K.F. Khaled, Electrochimica Acta, 55, 22, 2010, 6523-6532.

[4] Said Abbout, Meryem Zouarhi, Driss Chebabe, Mohamed Damej, Avni Berisha, Najat Hajjaji, Heliyon,6, 2020, e03574.

[5] Ohoud S. Al-Qurashi, Nuha Wazzan, Journal of Saudi Chemical Society, 26, 2022,

101566.

[6] X.Y. Zhang, Q.X. Kang, Y. Wang, Computational and Theoretical Chemistry, 1131, 2018,

25-32.

[7] A. H. Ahmed, M. El-Sayed Sherif, S. Hany Abdo, E. S. Gad, ACS Omega, 6, 2021, 14525-14532.

[8] A. S. Fouda, A. A. Ibrahim and W. T. El-behairy, Der Pharma Chemica, 2014, 6(5):144-157.

[9] S. Satarkar, R. S. Dubey. J. Sci. Res. 17 (2), 569-586 (2025)

[10] Altenpohl, D., & Zeiger, H. (1965). Corrosion. In aluminum. Springer. 19.

[11] Armijo, J. S. (1968). Corrosion, 24(1), 24-30.

[12] Berradja, A. (2019). Electrochemical Techniques for Corrosion and Tribocorrosion Monitoring: Fundamentals of Electrolytic Corrosion. Corrosion Inhibitors.

[13] Charng, T., & Lansing, F. (1982). Review of corrosion causes and corrosion control in a technical facility. Jet Propulsion Lab., Pasadena, CA (USA).

[14] Curley-Fiorino, M. E. & Schmid, G.M. (1980). The effect of the Cl− ion on the passive film on anodically polarized 304 stainless steel. Corrosion Science, 20(3), 313-329. https://doi.org/10.1016/0010-938X(80)90002-5

[15] Davis, J. R. (2001). Surface engineering for corrosion and wear resistance. ASM International, 279.

[16] Décarie, E. L., & Geider, R. J. (2017). Ecol Evol, 7(23), 10467-10481.

[17] Eliaz, N. (2019). Materials. 12(3),400-407.

[18] Evgueni, B., Nikolay P., & Boris S. (2004).. Phys. Rev. 70, 15-28.

[19] Fernandes, J. S., & Montenor, F. (2015). Corrosion. Materials For Construction And Civil Engineering, 2, 679-716.

[19] Giurlani & Innocenti, M. (2018). Electroplating for decorative applications: recent trends in research and development walter. Coatings, 8, 149-260.

[20] Goldstein, E. M. (1960). The Corrosion and oxidation of metals: scientific principles and practical applications. J. Chem. Educ. 37, 662-672.

[21] Hoar, T. P. (1949). Bulk metallic glasses: an overview. Trans. Faraday Soc. 45, 683-692.

[22] Hoar, T. P. & Agar, J. N. (1947). Factors in throwing power illustrated by potential-current diagrams. Discuss. Faraday Soc. 6-28.

[23 Jones, F. R. & Foreman, J. P. (2015). The response of aerospace composites to temperature and humidity in Polymer Composites in the Aerospace Industry. Woodhead Publishing, 335-369. https://doi.org/10.1016/B978-085709-523- 7.00012-8.

[24 Kabanov, B., Burstein, R. and Frumkin A. (1947). Pitting corrosion of metals – corrosion Discuss, Faraday Soc. NI. 254,12-26.

[25] Kadhim, M. G., & Albdiry, M. (2017). A critical review on corrosion and its prevention in the oilfield equipment. Journal of Petroleum Research and Study, 162-189.

[26] Kolotyrkin A. M. (2013). Pitting Corrosion of Metals. Corrosion, 19(8), 261-268. https://doi.org/10.5006/0010-9312- 19.8.261

[27] Kolotyrkin, J. M. (1963). Pitting corrosion of metals. Corrosion, 19(8). https://doi.org/10.5006/0010-9312-19.8.261

[28] Kolotyrkin, M., & Golovina, G.V. (1963). Pitting corrosion of metal, Acad. Sci. U.S.S.R. 148(106).

[29] Kumar, M., Kant, S., & Kumar, S., (2019). Corrosion behavior of wire arc sprayed Ni-based coatings in extreme environment. Materials Research Express, 6, 106427. https://doi.org/10.1088/2053-1591/ab3bd8

[30] Kumar, R., & Kumar, S. (2018). Comparative Parabolic Rate Constant and Coating Properties of Nickel, Cobalt, Iron and Metal Oxide Based Coating: A Review. I-manager's Journal on Material Sci. 6(1),45- 56. https://doi.org/10.26634/jms.6.1.14379.

[31] Kumar, R., & Kumar, S. (2018). Thermal Spray Coating Process: A Study. International Journal of Engineering Science and Research Technology, 7(3), 610-617.

[32] Kumar, R., Kumar, R., & Kumar, S. (2018). Erosion corrosion study of HVOF sprayed thermal sprayed coating on boiler tubes: a review. IJSMS. 1(3), 1-6.

[33] M. Taghavikish, N. Dutta, N. Roy Choudhury, Emerging Corrosion Inhibitors for Interfacial Coating, Coatings. 7 (2017) 217.

[34] Z. Khiati, Inhibition de la corrosion du cuivre en milieux chlorure et sulfate neutres par une nouvelle molécule dérivée de 1,2,4-triazole., (n.d.) 278.

[35] S. PAPAVINASAM__Corrosion Inhibitors // S Papavinasam Uhlig's Corrosion Handbook, 2011 Wiley Online Library

[36] M.G. Noack, EVALUATION OF CATALYZED HYDRAZINE AS AN OXYGEN SCAVENGER, Mater. Perform. 21 (1982) 26–31.

[37] D. Daoud, T. Douadi, S. Issaadi, S. Chafaa, Adsorption and corrosion inhibition of new synthesized thiophene Schiff base on mild steel X52 in HCl and H2SO4 solutions, Corrosion Science. 79 (2014) 50–58.

[38] K.F. Khaled, A. El-Maghraby, Experimental, Monte Carlo and molecular dynamics simulations to investigate corrosion inhibition of mild steel in hydrochloric acid solutions, Arabian Journal of Chemistry. 7 (2014) 319–326.

[39] X. Li, S. Deng, H. Fu, Three pyrazine derivatives as corrosion inhibitors for steel in 1.0M H2SO4 solution, Corrosion Science. 53 (2011) 3241–3247

[40] K.F. Khaled, Experimental and computational investigations of corrosion and corrosion inhibition of iron in acid solutions, Journal of Applied Electrochemistry. 41 (2011) 277–287.

[41] A.S. Fouda, H.A.A. Wahed, Corrosion inhibition of copper in HNO3 solution using thiophene and its derivatives, Arabian Journal of Chemistry. 9 (2016) S91–S99.

[42] Y. Qiang, L. Guo, S. Zhang, W. Li, S. Yu, J. Tan, Synergistic effect of tartaric acid with diaminopyridine on the corrosion inhibition of mild steel in 0.5 M HCl, Scientific Reports. 6 (2016).

[43] K.F. Khaled, The inhibition of benzimidazole derivatives on corrosion of iron in 1 M HCl solutions, Electrochimica Acta. 48 (2003) 2493–2503

[44] M. Boulkroune, A. Chibani, 2-Thiophene Carboxaldehyde as Corrosion Inhibitor for Zinc in Phosphoric Acid Solution, Chemical Science Transactions. 1 (2012) 355–364.

[45] A.B. Medrano-Solís, U. León-Silva, M.E. Nicho, 3-Thiophenemalonic acid as corrosion inhibitor of copper, Anti-Corrosion Methods and Materials. 64 (2017) 52–60.

[46] G. Gece, Theoretical evaluation of the inhibition properties of two thiophene derivatives

on corrosion of carbon steel in acidic media, Materials and Corrosion. (2012) 1-5.

[47] K.F. Khaled, N.S. Abdel-Shafi, N.A. Al-Mobarak, Understanding Corrosion Inhibition of iron by 2Thiophenecarboxylic Acid Methyl Ester: Electrochemical and Computational study, Int. J. Electrochem. Sci. 7 (2012) 18.

[48] A.S. Fouda, A.A. Attia, A.A. Negm, Some Thiophene Derivatives as Corrosion Inhibitors for Carbon Steel in Hydrochloric Acid, Journal of Metallurgy. 2014 (2014) 1–15.

[49] M. Bouklah, B. Hammouti, M. Benkaddour, T. Benhadda, Thiophene derivatives as effective inhibitors for the corrosion of steel in 0.5 m H2SO4, Journal of Applied Electrochemistry. 35 (2005) 1095–1101.

[42] S. Ben Aoun, Electrochemical Impedance Spectroscopy Investigations of Steel Corrosion in Acid media in the presence of Thiophene Derivatives, International Journal of Electrochemical Science. (2016) 7343–7358.

[50] M. Bouklah, B. Hammouti, A. Aouniti, T. Benhadda, Thiophene derivatives as effective inhibitors for the corrosion of steel in 0.5M H2SO4, Progress in Organic Coatings. 49, 225-228, 2004.

[51] Galal, N.F. Atta, M.H.S. Al-Hassan, Effect of some thiophene derivatives on the electrochemical behavior of AISI 316 austenitic stainless steel in acidic solutions containing chloride ions, Materials Chemistry and Physics. 89 (2005) 38–48.

[52] E. Schrödinger, Phys. Rev. 28, 1049, 1926.

[53] D.Born and Oppenheimar, J.R. Ann. Phys. Rev. 84, 457, 1927.

[54] D.R. Hartree, Proc. Cambridge Philos. Soc., 24 : 89, 1928.

[55] V. Fock. Z. Phys., 61 :126, 1930.

[56] K. Haddadi, Thèse de doctorat, université Sétif, 2013.

[57] N.Richard, CEA/DAM-Direction Ile de France, 2002

[58] L.H. Thomas, Proc. Cambridge Philos. Soc. 23, 542, 1928.

[59] E. Fermi. Z. Phys, 48 : i 3, 1928.

[60] P. Hohenberg and W. Kohn, Phys. Rev. B, 136, 864, 1964.

[61] W. Kohn and L.J. Sham, Phys. Rev. A 140, 1133, 1965.

[62] P. Geerlings, F. De Proft, and W. Langenaeker, Chem. Rev., 103, 1793, 2003.

[63] S.Chabbal. Thèse de doctorat, université de Toulouse 2010.

[64] R. M. Martin, Electronic structure Basic Theory and Practical Methods, Cambridge University Press, UK 2004.

[65] E. Betranhndy, Thèse de doctorat, université Bordeaux 1, 2005.

[66] P.A.M. Dirac, Proc. Cambridge Philos. Soc, 26, 376, 1930.

[67] J.C. Slater, Phys. Rev. 81, 385, 1951.

[68] K. Schwarz, Phys. Rev. B 5, 2466, 1972.

[69] D. M. Ceperley, B. J. Alder, Phys. Rev. Lett. 45, 566, 1980.

[70] G. Ortiz et P. Ballone. Phys. Rev. B, 50(3), 1994

[71] A.D .Becke, Phys. Rev. A, 38, 3098, 1988.

[72] J. P. Perdew, "In Electronic Structure of Solids ‘91" ; Ziesche P.and Eschrig H, 1991.

[73] J. P. Perdew, Phys. Rev. B. 33, 8822, 1986.

[74] C. Lee, W. Yang, R. G. Parr, Phys. Rev. B. 37, 785, 1988.